Checking the Influence of Sudden and Gradual Cooling Regimes on Strength, Near Surface Characteristics and Modulus of Elasticity of Hybrid Fibre Reinforced Blended Concretes Subjected to Sustained Elevated Temperatures Using Artificial Neural Networks

** Ashish A. Yaligar*
*** Shrikant B. Vanakudre*

Abstract

Prediction is made on strength, near surface characteristics, and modulus of elasticity of hybrid fibre reinforced blended concretes subjected to sustained elevated temperatures for 3 hours retention period using artificial neural networks (ANN). Temperature ranges from 100°C to 1000°C at an interval of 100°C and after that, specimens are subjected to two cooling regimes, that is, sudden and gradual. These specimens are subjected to tests for compressive strength, split tensile strength, water absorption, sorptivity, and modulus of elasticity. For building ANN models, available 440 experimental results produced with eight different mixture proportions are used. Two major artificial neural networks are used for prediction. One is for all the concrete combinations with sudden cooling [SCR] and other is with gradual cooling [GCR]. The data used in the multilayer feed forward neural network models (architecture, 8–15–1) is designed with eight input parameters covering temperature [T], cement [C], fly ash [FA], GGBFS [GGBFS] Silica Fume [SF], galvanized iron fibre [GIF] polypropylene fibre [PPF], and cooling regime [SCR or GCR]. These five tests are the outputs and they are predicted individually for both the cooling regimes. It shows that neural networks have high potential for predicting the results.

Keywords : **Artificial neural networks, cooling regime, modulus of elasticity, near surface characteristics, strength, sustained elevated temperatures.**

NOMENCLATURE

C	Cement.
FA	Fly Ash.
GGBFS	Ground Granulated Blast Furnace Slag.
SF	Silica Fume.
GIF	Galvanized Iron Fibre.
PPF	Polypropylene Fibre.
RT	Room Temperature.
IS	Indian Standards.
BS	British Standards.
ASTM	American Standard Test Method.
OPC	Ordinary Portland Cement.
ISO	International Organization for Standardization.
ASTM	American Society for Testing and Materials.
MPa	Mega Pascal.
ANN	Artificial Neural Networks.
HN	Hidden Neuron.
SCR	Sudden Cooling Regime.
GCR	Gradual Cooling Regime.
MSE	Mean Square Error.
RMSE	Root Mean Square Error.
f_{ce}	Experimental compressive strength in Mpa.
f_{cp}	Predicted compressive strength in Mpa.
f_{te}	Experimental split tensile strength in Mpa.
f_{tp}	Predicted split tensile strength in Mpa.
W_{ae}	Experimental water absorption in %

Manuscript received October 20, 2018; revised November 25, 2018; accepted November 17, 2018. Date of publication June 5, 2019.
* A. A. Yaligar is Assistant Professor with S. D. M. College of Engineering & Technology, Dharwad, Karnataka, India - 580 002. (email : ashishlgr@gmail.com)
** S. B. Vanakudre is Principal with S. D. M. College of Engineering & Technology, Dharwad, Karnataka, India - 580 002. (email : shrikantvanakudre@gmail.com)
DOI:10.17010/ijce/2019/v2i1/145716

W_{ap}	Predicted water absorption in %
S_e	Experimental sorptivity in mm/min$^{0.5}$.
S_p	Predicted sorptivity in mm/min$^{0.5}$.
E_{ce}	Experimental modulus of elasticity in Mpa.
E_{cp}	Predicted modulus of elasticity in Mpa.

I. INTRODUCTION

A. General

Life safety in case of fire is one of the major considerations in the design of structures. It is necessary to have complete knowledge about the behavior of all construction materials before using them in structural elements. The extensive use of concrete as a structural material in public utility buildings, multistorey buildings, exposed to the elements of terrorism necessitated the need to study the behavior of concrete at high temperature, and its durability for the required needs [1, 2].

Thermal property of concrete is an important aspect while dealing with durability of concrete structure exposed to elevated temperature. Damage to the structures depends on the intensity, duration of exposure, and also on the combustibility of the materials used in construction [3]. Concrete is incombustible, thus, giving it an advantage over materials like structural clay tile which expands much more rapidly than steel, and hence, tends to fail by reason of the destruction of the bond caused by unequal expansion. The rate of heat conductivity of concrete is very low, partly due to its porosity and consequent air content, and partly due to the dehydration of water. This later action increases the porosity and the conductivity of the concrete and leads to dehydration [4, 5].

Portland cement concrete is widely used in construction of buildings; it helps to satisfy the need for public safety in case of the fire hazards [6, 7], and also the addition of pozzolanas enhances the microstructure & phase composition when the concrete is under fire–resistance studies [8]. Similarly, addition of steel fibres helps to resist the pore pressure created and arrests the cracks and expansion, thus increasing the tensile strength. The addition of polypropylene fibres minimizes fire induced spalling of concrete [9]. Thus, it is necessitated to study the behavior of hybrid fibre reinforced blended concrete when subjected to high temperatures.

ANN technology, a sub–field of artificial intelligence is being used to solve a wide variety of problems in Civil Engineering applications [10–17]. The other important properties of ANN is its correct or nearly correct response to incomplete tasks, its extraction of information from noisy or poor data, and its production of generalized results from novel cases. These capabilities make ANN a very powerful tool to solve many civil engineering problems, particularly where data may be complex or in an insufficient amount [16]. The basic strategy for developing an ANN system based model for material behavior is to train an ANN system on the results of a series of experiments using that material [11–15]. If the experimental results include the relevant information about the material behavior, then the trained ANN system will contain enough information about behavior of the material to qualify as a material model [12–15]. Such a trained ANN system not only would be able to reproduce the experimental results, but it would also be able to approximate the results in other experiments through its generalization capability [11–15]. The ANN analysis was performed by using MATLAB 2013 software.

B. Objectives

The main objective of the research is to predict strength, near surface characteristics and modulus of elasticity of hybrid fibre reinforced blended concretes subjected to sustained elevated temperatures for 3 hours retention period using artificial neural networks (ANN).

The temperatures considered for the study were 30°C (RT), 100°C, 200°C, 300°C, 400°C, 500°C, 600°C, 700°C, 800°C, 900°C, and 1000°C. In this study, after the temperature application, specimens were subjected to two cooling regimes viz., sudden and gradual.

The concrete combinations used are listed in Table I. After the temperature test and cooling regimes, these specimens were tested for compressive strength [f_{ce}], split tensile strength [f_{te}], water absorption [W_{ae}], sorptivity [S_e], and modulus of elasticity [E_{ce}] tests.

By taking these experimental results, ANN analysis was performed as follows:

For building ANN models, available 440 experimental results produced with 8 different mixture proportions were used. Two major artificial neural networks were used for prediction. One was for all the concrete combinations with sudden cooling [SCR], and the other one was with gradual cooling [GCR]. The data used in the multilayer feed forward neural network models (architecture, 8–15–1) was designed with eight input parameters covering temperature [T], cement [C],

fly ash [FA], GGBFS [GGBFS], Silica Fume [SF], galvanized iron fibre [GIF], polypropylene fibre [PPF], and cooling regime [SCR or GCR]. Compressive strength [f_{cp}], split tensile strength [f_{tp}], water absorption [W_{ap}], sorptivity [S_p] and modulus of elasticity [E_{cp}] were the outputs, and they were predicted individually for both the cooling regimes.

II. EXPERIMENTAL AND ANALYTICAL PROGRAMME

A. Experimental Programme

1) Materials

Cement used was of OPC 43 grade and it satisfied the requirements of IS: 8112–2013 [18] (partially satisfies BS: 12–1996 [19] and ASTM C 150 / C 150M [20]). Laboratory test results are listed in Table II. Sand used was of grading zone II which met IS: 383–1970 [21] (partially satisfies BS: 882–1992 [22], and ASTM C 33 / C 33M [23]), and the properties are listed in Table III. Coarse aggregate (Greywacke) of 20 mm and down size was used and tested as per IS: 383–1970 (partially satisfied BS: 882–1992 and ASTM C 33 / C 33M), and the properties are listed in Table IV.

Mineral admixture used in this research was fly ash, GGBFS, and silica fume in which fly ash was brought from Raichur thermal power plant, Shaktinagar, Raichur, Karnataka, India, and tested as per IS 3812 (Part 1):2013 [24] (partially satisfied BS EN 450–1:2012 [25] and ASTM C 618–15 [26]). Its physical and chemical properties were mentioned in Table V and Table VI respectively. Similarly, GGBFS was procured from Mangalore, Karnataka, India and tested as per the requirements of IS 12089:1987 [27] (partially satisfied BS EN 15167–1:2006 [28], and ASTM C 989–04 [29]). Its physical and chemical properties are mentioned in Table VII and Table VIII respectively. Silica fume used was from Vadodara, Gujarat, India, which satisfied the requirements of IS 15388:2003[30] (partially satisfies BS EN 13263–1:2005 [31], and ASTM C 1240–15 [32]). Its physical and chemical properties are listed in Table IX and Table X respectively.

Two fibres were used in this research. Locally available galvanized iron wires were cut into straight fibres of length 50mm, thickness 1mm, and aspect ratio of 50. The properties of galvanized iron fibre are listed in Table XI. Polypropylene fibres were procured from Nagpur, India, and the properties are elaborated in Table XII.

To improve the workability and to reduce the water content, conplast SP430 superplasticizer was used, which confirmed to the requirements of IS 9103:1979 [33] (partially satisfied BS 5075–1:1982 [34], and ASTM C 494 / C 494M–16 [35]). The procured physical and chemical properties of superplasticizer are mentioned in Table XIII.

2) Experimental Procedure

Concrete is designed for M30 grade as per IS:

TABLE I.
CONCRETE COMBINATIONS USED IN THE EXPERIMENTS

Concrete Combinations	Blend percentage [*1]	Fibre Percentage [*2]	Remarks
C	100% Cement	-	Reference concrete
C + (GIF+PPF)	100% Cement	0.5% GIF + 0.5% PPF	Hybrid fibre reinforced reference concrete
(C+FA+GGBFS) + (GIF+PPF)	70% Cement + 15% Fly ash + 15% GGBFS	0.5% GIF + 0.5% PPF	Hybrid fibre reinforced ternary blended concrete 1
(C+FA+SF) + (GIF+PPF)	70% Cement + 15% Fly ash + 15% Silica fume	0.5% GIF + 0.5% PPF	Hybrid fibre reinforced ternary blended concrete 2

[*1]: Blends are calculated as percentage by weight of cementitious material.

[*2]: Fibre percentage is calculated from volume fraction method.

TABLE II.
PROPERTIES OF OPC 43 GRADE CEMENT (C)

Particulars	Test Results	Requirements as per IS: 8112-2013
Fineness (m^2/Kg) by Blaine's air permeability method	270	225 (Minimum)
Fineness (%) by dry sieving	4	
Specific Gravity	3.15	
Setting Time		
a. Initial (minutes)	60	30 (Minimum)
b. Final (minutes)	320	600 (Maximum)
Soundness by Le-chatelier's expansion method (mm)	2	10 (Maximum)
Soundness by Autoclave method expansion method (%)	0.2	0.8 (Maximum)
Compressive strength (MPa)		
a. 3 days	27	23 (Minimum)
b. 7 days	38	33 (Minimum)
c. 28 days	44	43 (Minimum)

TABLE III.
PROPERTIES OF FINE AGGREGATE

Particulars	Test Results	Requirements as per IS: 2386-1963
Organic impurities	Colourless	Colourless/Straw colour/Dark Colour
Silt content (%)	1.8	6-10% (Maximum)
Specific gravity	2.60	
Bulking of sand (%)	8.2	40% (Maximum)
Free moisture content	0.0	
Water Absorption (%)	1.0	
Bulk Density (Kg/m^3)		
a. Loose condition	1752.09	
b. Compacted condition	1827.12	
Fineness Modulus	2.88	

TABLE IV.
PROPERTIES OF COARSE AGGREGATE

Particulars	Test Results	Requirements as per IS: 2386-1963
Specific gravity	2.65	
Free moisture content (%)	0.0	
Water Absorption (%)	0.6	
Bulk Density (Kg/m^3)		
a. Loose condition	1782.64	
b. Compacted condition	1886.53	
Impact value (%)	15	30% (Maximum) used for concrete
Crushing value (%)	14.5	30% (Maximum) for surface course and 45% other than wearing course
Fineness Modulus	6.54	

TABLE V.
PHYSICAL PROPERTIES OF FLY ASH (FA)

Particulars	Test Results	Requirements as per IS: 3812 (Part 1)-2013
Fineness, specific surface area (m^2/kg) by Blaine's permeability method	333	320 (Minimum)
Particles retained on 45 micron IS sieve by Wet sieving (%)	4.52	34 (Maximum)
Specific Gravity	2.15	
Lime reactivity, average compressive strength (MPa)	4.68	4.5 (Minimum)
Compressive strength at 28 days (MPa)	23	Not less than 80% of the strength of corresponding plain cement mortar cubes
Soundness by autoclave test - Expansion of specimen (%)	0.2	0.8 (Maximum)

TABLE VI.
CHEMICAL PROPERTIES OF FLY ASH (FA)

Particulars	Test Results	Requirements as per IS: 3812 (Part 1)-2013
Silicon Dioxide (SiO_2) + Aluminium Oxide (Al_2O_3) + Iron Oxide (Fe_2O_3) in percent by mass	92.0	70 (Minimum)
Silicon dioxide (SiO_2) in percent by mass	62.6	35 (Minimum)
Reactive silica in percent by mass	38.2	20 (Minimum)
Magnesium oxide (MgO) in percent by mass	4.2	5.0 (Maximum)
Total sulphur as sulphur trioxide (SO_3) in percent by mass	2.6	3.0 (Maximum)
Available alkalis as equivalent sodium oxide (Na_2O) in percent by mass	Nil	1.5 (Maximum)
Total chlorides in percent by mass	0.01	0.05 (Maximum)
Loss on ignition in percent by mass	3.8	5.0 (Maximum)

TABLE VII.
PHYSICAL PROPERTIES OF GROUND GRANULATED BLAST FURNACE SLAG (GGBFS)

Particulars	Test Results	Requirements as per IS: 12089-1987
Fineness as specific surface m^2/Kg	350	275 (Minimum)
Compressive strength (MPa)		
a. 7 days	31.66	12 (Minimum)
b. 28 days	48.33	32.5 (Minimum)
Soundness, Le-Chatelier Expansion (mm)	0.0	10 (Maximum)
Initial setting time (min)	120	30 (Minimum)
Specific Gravity	2.85	

TABLE VIII.
CHEMICAL PROPERTIES OF GROUND GRANULATED BLAST FURNACE SLAG (GGBFS)

Particulars	Test Results	Requirements as per IS: 12089-1987
Insoluble residue (%)	0.41	1.5 (Maximum)
Magnesia Content (%)	7.55	14.0 (Maximum)
Sulphide content (%)	0.48	2.0 (Maximum)
Sulphite content (%)	0.44	2.5 (Maximum)
Loss on ignition (%)	0.33	3.0 (Maximum)
Manganese content (%)	0.12	2.0 (Maximum)
Chloride content (%)	0.011	0.10 (Maximum)
Glass content (%)	93	67 (Minimum)
Chemical Modulus		
a. $CaO+MgO+SiO_2$	77.14	66.66 (Minimum)
b. $CaO+MgO+SiO_2$	1.33	1.0 (Minimum)
c. CaO/SiO_2	1.10	1.40 (Maximum)

TABLE IX.
PHYSICAL PROPERTIES OF SILICA FUME (SF)

Particulars	Test Results	Requirements as IS: 15388-2003
Specific surface m^2/g	20	15 (Minimum)
Oversize % retained on 45 micron IS Sieve	3.6	10 (Maximum)
Oversize % retained on 45 micron IS Sieve variation from average %	1.8	5 (Maximum)
Compressive strength at 7 days (MPa)	26	Not less than 85 percent of the strength of Control Sample
Specific Gravity	2.2	
Bulk density (kg/m^3)	640	500 to 700
Colour	Black	

TABLE X.
CHEMICAL PROPERTIES OF SILICA FUME (SF)

Particulars	Test Results	Requirements as per IS: 15388-2003
SiO_2 (%)	90.3	85 (Minimum)
Moisture content (%)	0.7	3 (Maximum)
Loss of ignition @ 975^oC (%)	2.1	6 (Maximum)
Carbon (%)	0.85	2.5 (Maximum)
Alkalies as Na_2O (%)	0.3	1.5 (Maximum)

TABLE XI.
PROPERTIES OF GALVANIZED IRON FIBRE (GIF)

Particulars	Properties
Shape	Straight
Length (mm)	50
Diameter (mm)	1
Aspect ratio	50
Density (Kg/m^3)	7850
Maximum Tensile strength (MPa)	825
Appearance	Bright and clean white

TABLE XII.
PROPERTIES OF POLYPROPYLENE FIBRE (PPF)

Particulars	Properties
Specific Gravity	0.91
Alkali Resistance	Alkali Proof
Chemical Resistance	Excellent
Acid & Salt Resistance	Chemical Proof
Denier	1050
Tensile Strength (kN/mm^2)	0.67
Young's Modulus (kN/mm^2)	4.00
Melt Point	165
Ignition Point	600
Absorption	Nil
Density-Bulk (Kg/m^3)	910
Density-Loose (Kg/m^3)	250-430
Fibre Cut Length (mm)	20
Form	Fibrillated (Mesh)
Colour	Natural white
Dispersion	Excellent

TABLE XIII.
PHYSICAL AND CHEMICAL PROPERTIES OF SUPERPLASTICIZER

Particulars	Properties
Specific Gravity	1.22
Physical state	Liquid
Chloride content	Nil
Air entrainment	1%
Colour	Brown
Odour	Slight/faint
pH (Concentrate)	7-8
Boiling point (°C)	>100
Flash point, closed (°C)	None
Vapour pressure (kPa @ 20°C)	2.3
Relative density (@ 20°C)	1.2
Water solubility	Soluble
Dosage	0.5-2.0 litre/100 Kg cement

10262–2009 [36]. Based on several trials, the water–cement ratio arrived at was 0.45 and 100mm slump was maintained. The mix proportion 1: 2.02: 3.45 was obtained. The blends are calculated as percentage by weight of cementitious material and fibres by volume fraction method [37].

For assessing compressive strength and near surface characteristics (water absorption & sorptivity), 264 standard cube specimens of 150 mm were cast. For split tensile strength, 264 standard cylinder specimens of 150 mm diameter and 300 mm height were cast, and similar 264 standard cylinders were also cast to test modulus of elasticity. Specimens were allowed to cure for 28 days.

The fire test was conducted at Udyambag, Belagavi,

Karnataka, India. A pit type electrical furnace buried inside the ground consisting of elements of Kanthal wire giving electrical load of 32kW was used. The maximum temperature inside the furnace was 1200°C. Furnace was cylindrical in shape having 400 mm diameter and 1.2 m deep, having control panel with temperature indicator, temperature sensor, and ampere rating. According to ISO 834 [38], and ASTM E119, the standard time-temperature (t-T) curve is as shown in Fig. 1. In this research, the t-T curve used for the furnace is shown in Fig. 2. The concrete specimens were kept inside the furnace for a retention period of 3 hours [39].

After temperature test and cooling regimes, the specimens were subjected to compressive strength [f_{ce}] as per IS: 516–1959 [40], (partially satisfies BS 1881–116:1983[41], and ASTM C 39 / C 39M[42]), split

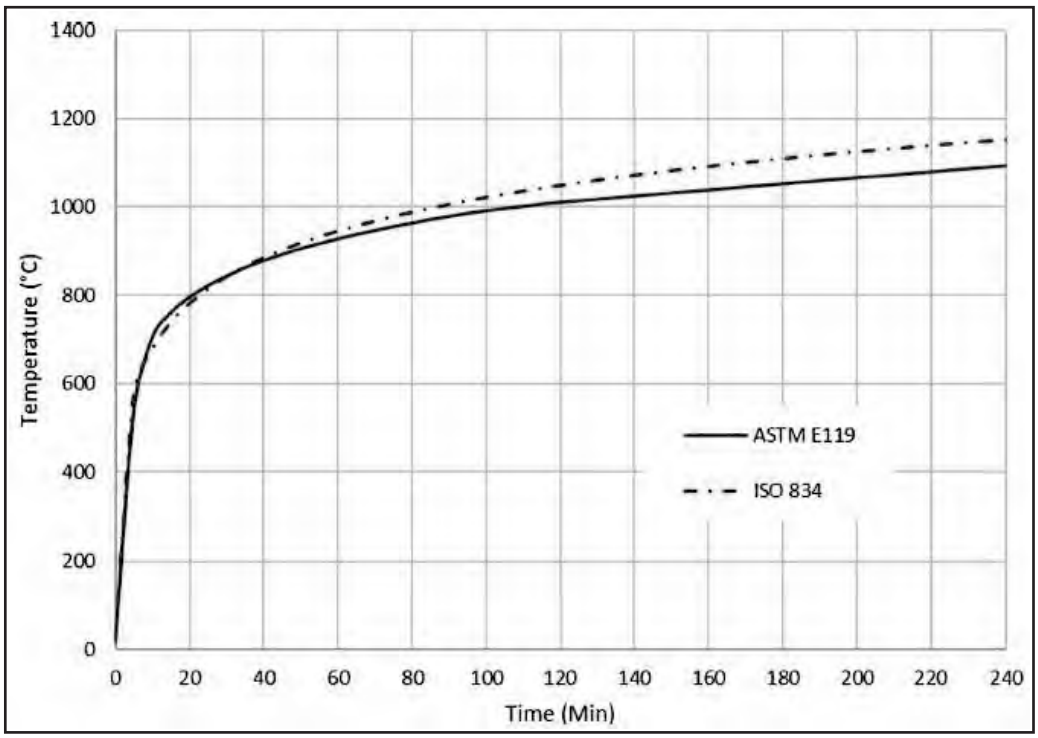

Fig. 1. Standard t-T Curve according to ISO 834 and ASTM E119

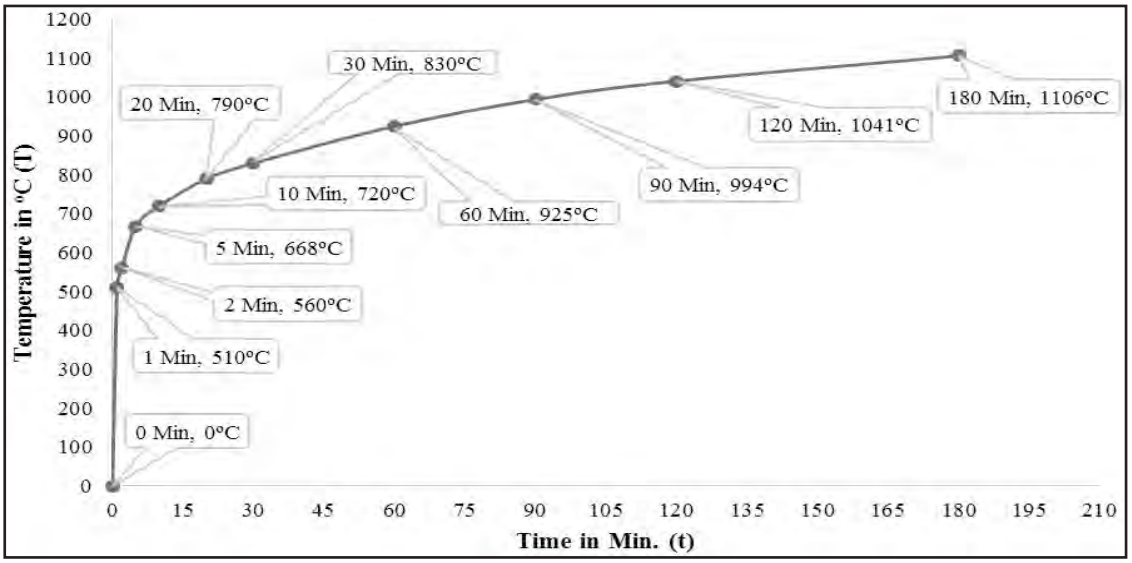

Fig. 2. Time-temperature (t-T) curve used in the furnace

tensile strength [f_{te}] as per IS: 5816–1999 [43] (partially satisfied BS 1881 (Part 117): 1983 [44] and ASTM C 496 / C 496M – 11 [45]), for near surface characteristics (water absorption [W_{ae}] & sorptivity [S_e]) [46], and modulus of elasticity [E_{ce}] as per IS: 516–1959 [40], (partially satisfies ASTM C 469 / C 469M–14 [47]).

B. Analytical Programme

1) Artificial Neural Networks

ANNs are computing systems made up of a number of simple, highly interconnected processing elements which process information by their dynamic state response to external inputs [48]. The fundamental concept of neural networks is the structure of the information processing system [15]. Generally, an ANN are made of an input layer of neurons, sometimes referred to as nodes or processing units, one or several hidden layers of neurons and output layers of neurons. The neighbouring layers are fully interconnected by weight. The input layer neurons receive information from the outside environment and transmit them to the neurons of the hidden layer without performing any calculation [49, 50]. Layers between the input and output layers are called hidden layers, and may contain a large number of hidden processing units [17]. All problems that can be solved by a perceptron can be solved with only one hidden layer, but it is sometimes more efficient to use two or three hidden layers. Finally, the output layer neurons produce the network predictions to the outside world [49, 50]. Each neuron of a layer other than the input layer computes first a linear combination of the outputs of the neurons of the previous layer, plus a bias. The coefficients of the linear combinations plus the biases are called weights.

Neurons in the hidden layer then compute a nonlinear function of their input. Generally, the nonlinear function is the sigmoid function [15]. According to the information mentioned here, an artificial neuron is composed of five main parts: inputs, weights, sum function, activation function and output. Fig. 3 shows a typical neural network with input, sum function, sigmoid activation function and output.

The input to a neuron from another neuron is obtained by multiplying the output of the connected neuron by the synaptic strength of the connection between them [51]. The weighted sums of the input components $(net)_j$ are calculated in (1):

$$(net)_j = \Sigma^n_{i=1} W_{ij} O_i + i \qquad (1)$$

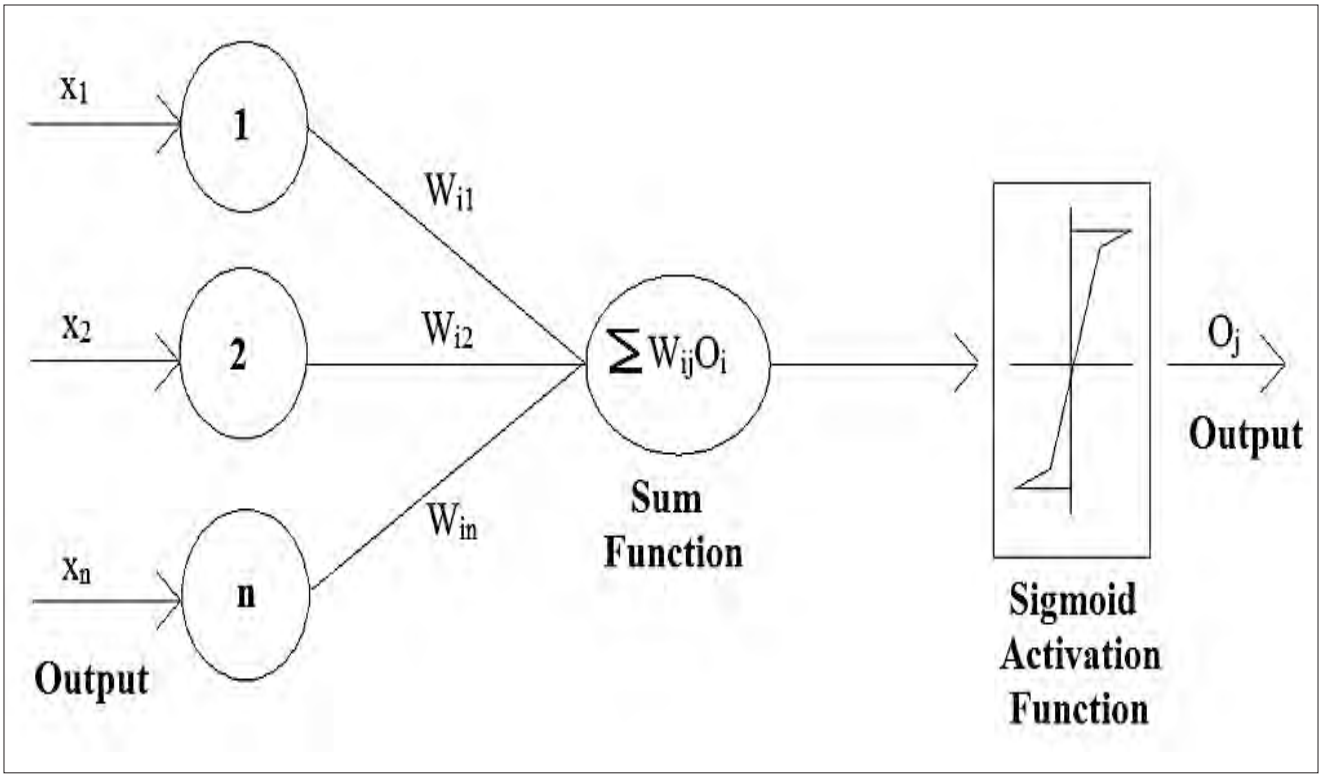

Fig. 3. Artificial Neuron Model

Here, $(net)_j$ is the weighted sum of the j^{th} neuron for the input received from the preceding layer with n neurons, W_{ij} is the weight between the j^{th} neuron in the preceding layer, O_i is the output of the i^{th} neuron in the preceding layer [12–14]. The quantity b is called the bias and is used to model the threshold. The output signal of the neuron, denoted by O_j in Fig. 3 is related to the network input $(net)_j$ via a transformation function called the activation function [18].

The most common activation functions are ramp, sigmoid, and Gaussian functions. In general, for multilayer receptive models, the activation function $(f(net)_j)$ sigmoid function is used. The output of the j^{th} neuron O_j is calculated by (2) with a sigmoid function as follows [12–14] :

$$O_j = f(net)_j = \frac{1}{1+e^{-\alpha (net)_j}} \qquad (2)$$

Here O_j is the output of neuron, α is a constant used to control the slope of the semi–linear region. The sigmoid nonlinearity activates in every layer except in the input layer [13, 14, 51]. The sigmoid function represented by (2) gives outputs in (0, 1) [12–14]. In recent years, ANNs have been applied to many civil engineering problems with some degree of success. In civil engineering, neural networks have been applied to the detection of structural damage, structural system identification, modeling of material behavior, structural optimization, structural control, ground water monitoring, prediction of experimental studies, and concrete mix proportions [17]. Neural network based modelling process determination includes: (a) data acquisition, analysis and problem representation; (b) architecture determination; (c) learning process determination; (d) training of the networks; and (e) testing of the trained network for generalization evaluation [14, 52]. After these processes are carried out, ANN can supply meaningful answers even when the data to be processed include errors or are incomplete and can process information extremely rapidly when applied to solve engineering problems [14, 53].

2) Feed Forward Networks

In a multilayer feed forward neural network, the artificial neurons are arranged in layers, and all the neurons in each layer have connections to all the neurons in the next layer [15]. However, there is no connection between neurons of the same layer or the neurons which are not in successive layers. The multilayer feed forward network consists of one input layer, one or two hidden layers and one output layer of neurons [51]. Associated with each connection between these artificial neurons, a weight value is defined to represent the connection weight [15]. Fig. 4 shows a typical architecture of a multilayer feed forward neural network with an input layer, hidden layer, and an output layer. The input layer receives input information, and passes it onto the neurons of the hidden layer (s), which in turn pass the information to the output layer.

The output from the output layer is the prediction of the net for the corresponding input supplied at the input nodes. Each neuron in the network behaves in the same way as discussed in (1) and (2). There is no reliable method for deciding the number of neural units required for a particular problem. This is decided based on experience and a few trials are required to determine the best configuration of the network [18]. In this study, the multilayer feed forward type of ANN, is shown in Fig. 4 is considered. In a multilayer feed forward network, the inputs and output variables are normalized within the range of 0–1.

3) The Back Propagation Algorithm

Back propagation algorithm, one of the most well–known training algorithms is a gradient descent

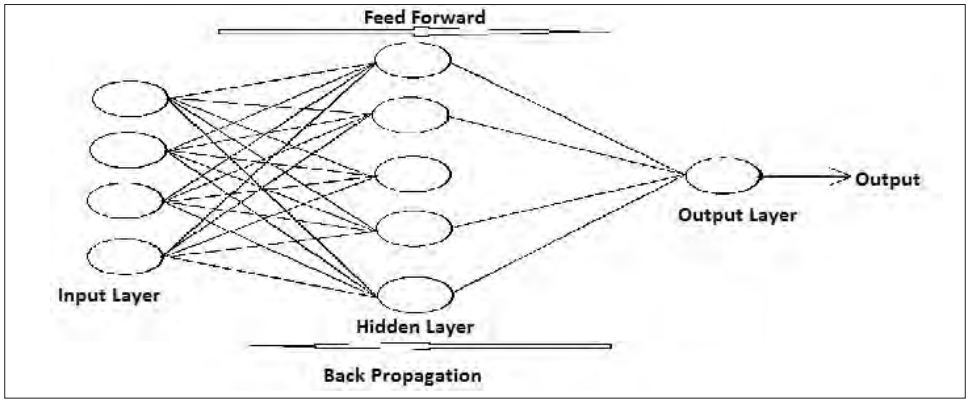

Fig. 4. Typical Architecture of a Multilayer Feed Forward Neural Network

technique to minimize the error for a particular training pattern in which it adjusts the weights by a small amount at a time [12–14]. The network error is passed backwards from the output layer to the input layer, and the weights are adjusted based on some learning strategies so as to reduce the network error to an acceptable level [49]. The error for r^{th} example is calculated in (3):

$$E_r = \frac{1}{2}(t_j - O_j)^2 \qquad (3)$$

Here, t_j is the output desired at neuron j and O_j is the output predicted at neuron j. As presented in (1) and (2), the output O_j is a function of synaptic strength and outputs of the previous layer [51]. The learning consists of changing the weights in order to minimize this error function in a gradient descent technique. In the back propagation phase, the error between the network output and the desired output values is calculated using the so–called generalized delta rule [54], and weights between neurons are updated from the output layer to the input layer by as shown in (4) [16].

$$W_{ij}(m+1) = W_{ij}(m) + \eta(\delta_j O_j) + \beta w_{ij}(t) \qquad (4)$$

Here, the δ_j is the error signal at a neuron j, O_j is the output of neuron j, m is the number of iteration, and η, β are called learning rate and momentum rate, respectively. δ_j in (4) can be calculated using the partial derivative of the error function E_r in the output layer and other layer, respectively, by (5) and (6) [16, 51].

$$\delta_j = O_j(t_j - O_j)(1 - O_j) \qquad (5)$$

$$\delta_j = O_j(1 - O_j)\Sigma\delta_k W_{kj} \qquad (6)$$

Here, the k^{th} layer means the upper layer of the j^{th} layer [16]. These operations are repeated for each example, and for all the neurons until a satisfactory convergence is achieved for all the examples present in the training set [51]. The training process is successfully completed when the iterative process has converged. The connection weights are captured from the trained network in order to use them in the recall phase [16]. For the present study, a multilayer feed forward network was adopted for training purpose. The error was reduced using a back propagation algorithm.

4) Neural Network Models

In this study, a multilayer feed forward neural network with a back propagation algorithm was adopted. The nonlinear sigmoid function was used in the hidden layer and the cell outputs at the output layer. Momentum rate was taken as 0.7, learning rate was 0.3, error after learning was 0.001, and learning cycles were 1000. For building ANN models, available 440 experimental results produced with 8 different mixture proportions were used. The neural network model architecture was 8–15–1. As shown in Fig. 5(a) and 5(b), two artificial neural networks were used for prediction.

One is for all the concrete combinations with sudden cooling [SCR] and other one is with gradual cooling [GCR]. The data used in the multilayer feed forward neural network models are designed with eight inputs. The first model includes T, C, FA, GGBFS, SF, GIF, PPF with SCR and the other one includes T, C, FA, GGBFS, SF, GIF, PPF with GCR. f_{cp}, f_{tp}, W_{ap}, S_p, and E_{cp} are the outputs and they are predicted individually as shown in Table XIV for both the cooling regimes.

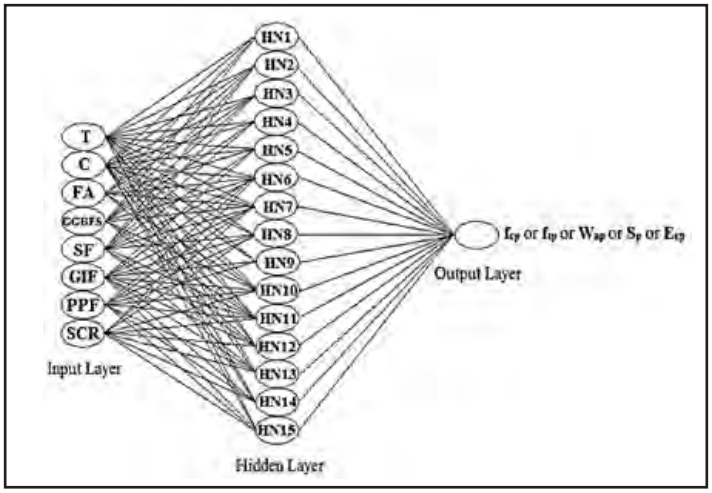

(a)

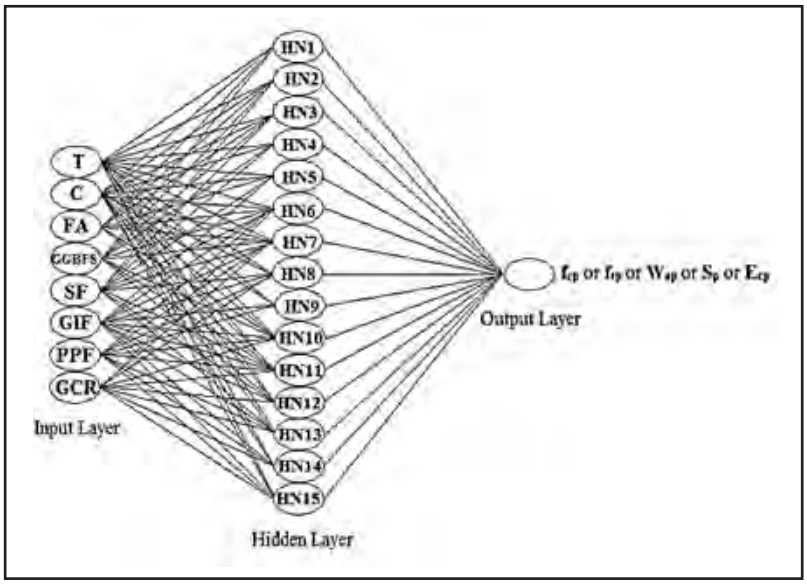

(b)

Fig. 5. System used in ANN Model for (a) Sudden Cooling Regime (SCR) and (b) Gradual Cooling Regime (GCR)

One is for all the concrete combinations with sudden cooling [SCR] and other one is with gradual cooling [GCR]. The data used in the multilayer feed forward neural network models are designed with eight inputs. The first model includes T, C, FA, GGBFS, SF, GIF, PPF with SCR and the other one includes T, C, FA, GGBFS, SF, GIF, PPF with GCR. f_{cp}, f_{tp}, W_{ap}, S_p, and E_{cp} are the outputs and they are predicted individually as shown in Table XIV for both the cooling regimes.

III. RESULTS AND DISCUSSION

In each ANN models, 44 data of experiment results were used. 70% data of experiment results were used for training whereas, 15% were employed for validation and 15% for testing. In ANN models, one hidden layer was selected. In the hidden layer 15 neurons were determined due to its minimum absolute percentage error values for training and testing sets. The limit values of input and output variables used in models are listed in Table XV. In the ANN models, the neurons of neighbouring layers are fully interconnected by weights. Finally, the output layer neuron produces the network prediction as a result.

Table XVI represents the data used in model construction for all the concrete combinations with sudden cooling regime (Model No. 1, 3, 5, 7, 9). Table XVII represents data used in model construction for all the concrete combinations with gradual cooling regime

TABLE XIV.
ANN MODEL ARCHITECTURES

Model Sl. No.	Input Layer Neurons (8)	Hidden Layer Neurons (15)	Output Layer Neurons (1)
1	T, C, FA, GGBFS, SF, GIF, PPF, SCR	HN 1 to HN 15	f_{cp}
2	T, C, FA, GGBFS, SF, GIF, PPF, GCR	HN 1 to HN 15	f_{cp}
3	T, C, FA, GGBFS, SF, GIF, PPF, SCR	HN 1 to HN 15	f_{tp}
4	T, C, FA, GGBFS, SF, GIF, PPF, GCR	HN 1 to HN 15	f_{tp}
5	T, C, FA, GGBFS, SF, GIF, PPF, SCR	HN 1 to HN 15	W_{ap}
6	T, C, FA, GGBFS, SF, GIF, PPF, GCR	HN 1 to HN 15	W_{ap}
7	T, C, FA, GGBFS, SF, GIF, PPF, SCR	HN 1 to HN 15	S_p
8	T, C, FA, GGBFS, SF, GIF, PPF, GCR	HN 1 to HN 15	S_p
9	T, C, FA, GGBFS, SF, GIF, PPF, SCR	HN 1 to HN 15	E_{cp}
10	T, C, FA, GGBFS, SF, GIF, PPF, GCR	HN 1 to HN 15	E_{cp}

TABLE XV.

THE INPUT AND OUTPUT QUANTITIES USED IN ANN MODELS

Input Variables	Data used in Training and Testing the Models			
	Sudden Cooling [SCR]		Gradual Cooling [GCR]	
	Minimum	Maximum	Minimum	Maximum
Sustained Elevated Temperature (°C) [T]	30	1000	30	1000
Cement (Kg/m^3) [C]	245.35	350.51	245.35	350.51
Fly Ash (Kg/m^3) [FA]	0.00	52.58	0.00	52.58
GGBFS (Kg/m^3)	0.00	52.58	0.00	52.58
Silica Fume (Kg/m^3) [SF]	0.00	52.58	0.00	52.58
GIF (%)	0	0.5	0	0.5
PPF (%)	0	0.5	0	0.5
Cooling Regime [SCR or GCR]	1	1	2	2
Output Variables	**Data used in Training and Testing the Models**			
	Sudden Cooling [SCR]		Gradual Cooling [GCR]	
	Minimum	Maximum	Minimum	Maximum
Compressive Strength (MPa) [f_{ce}]	8.30	54.92	10.12	55.18
Split Tensile Strength (MPa) [f_{te}]	0.00	6.18	0.12	6.28
Water Absorption (%) [W_{ae}]	0.93	5.60	0.92	5.45
Sorptivity (mm/min$^{0.5}$) [S_e]	15.50	2.52	15.18	2.47
Modulus of Elasticity x 104 (MPa) [E_{ce}]	0.60	4.78	0.72	4.81

(Model No. 2, 4, 6, 8, 10).

Table XVIII represents the comparison of experimental and ANN predicted compressive strength results for all the concrete combinations with sudden cooling regime (Model No. 1) and gradual cooling regime (Model No. 2). The percentage error is also shown. Fig. 6 shows the comparison of experimental and ANN predicted compressive strength results for all the concrete combinations with (a) sudden cooling (Model No. 1) and (b) gradual cooling (Model No. 2). Linear regression equations are also shown for each concrete combination.

Table XIX represents comparison of experimental and ANN predicted split tensile strength results for all the concrete combinations with sudden cooling regime (Model No. 3) and gradual cooling regime (Model No. 4). The percentage error is also shown. Fig. 7 shows comparison of experimental and ANN predicted split tensile strength results for all the concrete combinations with (a) sudden cooling (Model No. 3) and (b) gradual cooling (Model No. 4). Linear regression equations are also shown for each concrete combination.

Table XX represents comparison of experimental and ANN predicted water absorption results for all the concrete combinations with sudden cooling regime (Model No. 5) and gradual cooling regime (Model No. 6). The percentage error is also shown in Fig. 8, it shows comparison of experimental and ANN predicted water absorption results for all the concrete combinations with (a) sudden cooling (Model No. 5) and (b) gradual cooling (Model No. 6). Linear regression equations are also shown for each concrete combination.

Table XXI represents comparison of experimental and ANN predicted sorptivity results for all the concrete combinations with sudden cooling regime (Model No. 7), and gradual cooling regime (Model No. 8). The percentage error is also shown. Fig. 9 shows comparison of experimental and ANN predicted sorptivity results for all the concrete combinations with (a) sudden cooling (Model No. 7) and (b) gradual cooling (Model No. 8). Linear regression equations are also shown for each concrete combination.

Table XXII represents comparison of experimental and ANN predicted modulus of elasticity results for all the concrete combinations with sudden cooling regime (Model No. 9), and gradual cooling regime (Model No. 10). The percentage error is also shown. Fig. 10 shows comparison of experimental and ANN predicted modulus of elasticity results for all the concrete combinations with (a) sudden cooling (Model No. 9) and

(b) gradual cooling (Model No. 10). Linear regression equations are also shown for each concrete combination.

In this study, error arising during training and testing in ANN models can be expressed as a mean squared error (MSE) and is calculated by in (7) [13, 14].

$$\text{MSE} = \frac{1}{n} \Sigma_i |t_i - O_i|^2 \quad (7)$$

In addition, root–mean squared error (RMSE) and the absolute fraction of variance (R^2) are calculated in (8) and (9), respectively [13, 14, 55, 56].

$$\text{RMSE} = \sqrt{\frac{1}{n} \Sigma_i |t_i - O_i|^2} \quad (8)$$

$$R^2 = 1 - \left[\frac{\Sigma_i (t_i - O_i)^2}{\Sigma_i (O_i)^2} \right] \quad (9)$$

Here t is the target value, O is the output value, n is the pattern. The statistical values for all the stations such as MSE, RMSE and R^2 for training, validating and testing are given in Table XXIII for each output with both the regimes.

It is observed that MSE, RMSE and R^2 values for all the 10 ANN models are within the permissible limits (MSE, RMSE $\cong$ 0 and $R^2 \cong 1$). The trained models were only tested with the input values and the results found were close to experiment results.

TABLE XVI.
DATA USED IN MODEL CONSTRUCTION FOR ALL THE CONCRETE COMBINATIONS WITH SUDDEN COOLING REGIME

	Data Used in Model Construction							
Combination	**Sustained Elevated Temperature (°C) [T]**	**Cement (Kg/m³) [C]**	**Fly Ash (Kg/m³) [FA]**	**GGBFS (Kg/m³)**	**Silica Fume (Kg/m³) [SF]**	**GIF (%)**	**PPF (%)**	**Sudden Cooling Regime [SCR]**
C, Sudden Cooling	30	350.51	0	0	0	0	0	1
	100	350.51	0	0	0	0	0	1
	200	350.51	0	0	0	0	0	1
	300	350.51	0	0	0	0	0	1
	400	350.51	0	0	0	0	0	1
	500	350.51	0	0	0	0	0	1
	600	350.51	0	0	0	0	0	1
	700	350.51	0	0	0	0	0	1
	800	350.51	0	0	0	0	0	1
	900	350.51	0	0	0	0	0	1
	1000	350.51	0	0	0	0	0	1
C + (GIF+PPF),	30	350.51	0	0	0	0.5	0.5	1
Sudden Cooling	100	350.51	0	0	0	0.5	0.5	1
	200	350.51	0	0	0	0.5	0.5	1
	300	350.51	0	0	0	0.5	0.5	1
	400	350.51	0	0	0	0.5	0.5	1
	500	350.51	0	0	0	0.5	0.5	1

	600	350.51	0	0	0	0.5	0.5	1
	700	350.51	0	0	0	0.5	0.5	1
	800	350.51	0	0	0	0.5	0.5	1
	900	350.51	0	0	0	0.5	0.5	1
	1000	350.51	0	0	0	0.5	0.5	1
(C+FA+GGBFS) +	30	245.35	52.58	52.58	0	0.5	0.5	1
GIF+PPF),	100	245.35	52.58	52.58	0	0.5	0.5	1
Sudden Cooling	200	245.35	52.58	52.58	0	0.5	0.5	1
	300	245.35	52.58	52.58	0	0.5	0.5	1
	400	245.35	52.58	52.58	0	0.5	0.5	1
	500	245.35	52.58	52.58	0	0.5	0.5	1
	600	245.35	52.58	52.58	0	0.5	0.5	1
	700	245.35	52.58	52.58	0	0.5	0.5	1
	800	245.35	52.58	52.58	0	0.5	0.5	1
	900	245.35	52.58	52.58	0	0.5	0.5	1
	1000	245.35	52.58	52.58	0	0.5	0.5	1
(C+FA+SF) + (GIF+PPF),	30	245.35	52.58	0	52.58	0.5	0.5	1
Sudden Cooling	100	245.35	52.58	0	52.58	0.5	0.5	1
	200	245.35	52.58	0	52.58	0.5	0.5	1
	300	245.35	52.58	0	52.58	0.5	0.5	1
	400	245.35	52.58	0	52.58	0.5	0.5	1
	500	245.35	52.58	0	52.58	0.5	0.5	1
	600	245.35	52.58	0	52.58	0.5	0.5	1
	700	245.35	52.58	0	52.58	0.5	0.5	1
	800	245.35	52.58	0	52.58	0.5	0.5	1
	900	245.35	52.58	0	52.58	0.5	0.5	1
	1000	245.35	52.58	0	52.58	0.5	0.5	1

TABLE XVII.
DATA USED IN MODEL CONSTRUCTION FOR ALL THE CONCRETE COMBINATIONS WITH GRADUAL COOLING REGIME

Combination	Data used in Model Construction							
	Sustained Elevated Temperature (°C) [T]	Cement (Kg/m^3) [C]	Fly Ash (Kg/m^3) [FA]	GGBFS (Kg/m^3)	Silica Fume (Kg/m^3) [SF]	GIF (%)	PPF (%)	Gradual Cooling Regime [GCR]
C, Gradual Cooling	30	350.51	0	0	0	0	0	2
	100	350.51	0	0	0	0	0	2
	200	350.51	0	0	0	0	0	2
	300	350.51	0	0	0	0	0	2
	400	350.51	0	0	0	0	0	2
	500	350.51	0	0	0	0	0	2
	600	350.51	0	0	0	0	0	2
	700	350.51	0	0	0	0	0	2
	800	350.51	0	0	0	0	0	2
	900	350.51	0	0	0	0	0	2
	1000	350.51	0	0	0	0	0	2

C + (GIF+PPF),	30	350.51	0	0	0	0.5	0.5	2
Gradual Cooling	100	350.51	0	0	0	0.5	0.5	2
	200	350.51	0	0	0	0.5	0.5	2
	300	350.51	0	0	0	0.5	0.5	2
	400	350.51	0	0	0	0.5	0.5	2
	500	350.51	0	0	0	0.5	0.5	2
	600	350.51	0	0	0	0.5	0.5	2
	700	350.51	0	0	0	0.5	0.5	2
	800	350.51	0	0	0	0.5	0.5	2
	900	350.51	0	0	0	0.5	0.5	2
	1000	350.51	0	0	0	0.5	0.5	2
(C+FA+GGBFS) +	30	245.35	52.58	52.58	0	0.5	0.5	2
GIF+PPF),	100	245.35	52.58	52.58	0	0.5	0.5	2
Gradual Cooling	200	245.35	52.58	52.58	0	0.5	0.5	2
	300	245.35	52.58	52.58	0	0.5	0.5	2
	400	245.35	52.58	52.58	0	0.5	0.5	2
	500	245.35	52.58	52.58	0	0.5	0.5	2
	600	245.35	52.58	52.58	0	0.5	0.5	2
	700	245.35	52.58	52.58	0	0.5	0.5	2
	800	245.35	52.58	52.58	0	0.5	0.5	2
	900	245.35	52.58	52.58	0	0.5	0.5	2
	1000	245.35	52.58	52.58	0	0.5	0.5	2
(C+FA+SF) + (GIF+PPF),	30	245.35	52.58	0	52.58	0.5	0.5	2
Gradual Cooling	100	245.35	52.58	0	52.58	0.5	0.5	2
	200	245.35	52.58	0	52.58	0.5	0.5	2
	300	245.35	52.58	0	52.58	0.5	0.5	2
	400	245.35	52.58	0	52.58	0.5	0.5	2
	500	245.35	52.58	0	52.58	0.5	0.5	2
	600	245.35	52.58	0	52.58	0.5	0.5	2
	700	245.35	52.58	0	52.58	0.5	0.5	2
	800	245.35	52.58	0	52.58	0.5	0.5	2
	900	245.35	52.58	0	52.58	0.5	0.5	2
	1000	245.35	52.58	0	52.58	0.5	0.5	2

TABLE XVIII.
COMPARISON OF EXPERIMENTAL AND ANN PREDICTED COMPRESSIVE STRENGTH RESULTS FOR ALL THE CONCRETE COMBINATIONS WITH BOTH COOLING REGIMES

		Compressive Strength				Compressive Strength		
Sustained Elevated Temperature (°C) [T]	**Combination**	**Experimental Result (MPa) [f_{ce}]**	**Predicted Result (MPa) [f_{cp}]**	**% Error**	**Combination**	**Experimental Result (MPa) [f_{ce}]**	**Predicted Result (MPa) [f_{cp}]**	**% Error**
30	C, Sudden Cooling	39.53	37.797	1.733	C, Gradual Cooling	39.97	37.872	2.098
100		38.64	38.323	0.317		39.08	39.075	0.005
200		37.68	38.588	-0.908		38.18	39.175	-0.995

300		36.86	37.020	-0.160		37.30	37.291	0.009
400		33.82	33.730	0.090		34.25	34.061	0.189
500		29.86	29.576	0.284		30.30	30.239	0.061
600		25.33	25.223	0.107		26.20	26.341	-0.141
700		21.19	20.904	0.286		22.64	22.532	0.108
800		16.85	16.554	0.296		17.80	18.727	-0.927
900		12.30	11.980	0.320		14.75	14.766	-0.016
1000		8.30	6.984	1.316		10.12	10.514	-0.394
30	C + (GIF+PPF),	46.81	46.767	0.043	C + (GIF+PPF),	47.32	47.390	-0.070
100	Sudden Cooling	46.25	46.017	0.233	Gradual Cooling	46.78	46.579	0.201
200		45.15	45.241	-0.091		45.68	45.881	-0.201
300		44.10	43.934	0.166		44.60	44.462	0.138
400		40.36	40.942	-0.582		40.82	41.288	-0.468
500		36.00	36.333	-0.333		36.45	36.721	-0.271
600		31.30	31.191	0.109		31.67	31.704	-0.034
700		26.60	26.312	0.288		26.92	26.808	0.112
800		21.80	21.799	0.001		22.06	22.102	-0.042
900		17.20	17.357	-0.157		17.40	17.414	-0.014
1000		12.50	12.656	-0.156		12.63	12.589	0.041
30	(C+FA+GGBFS) + (GIF+PPF),	54.14	54.641	-0.501	(C+FA+GGBFS) +	54.72	54.604	0.116
100	Sudden Cooling	53.60	54.203	-0.603	(GIF+PPF),	54.20	54.346	-0.146
200		52.95	53.477	-0.527	Gradual Cooling	53.60	53.766	-0.166
300		52.35	52.253	0.097		52.98	52.564	0.416
400		49.72	50.297	-0.577		50.32	50.478	-0.158
500		46.88	47.641	-0.761		47.45	47.633	-0.183
600		44.12	44.279	-0.159		44.65	44.459	0.191
700		40.35	40.137	0.213		40.84	40.942	-0.102
800		36.15	35.486	0.664		36.55	36.516	0.034
900		31.50	30.603	0.897		31.84	30.977	0.863
1000		27.32	25.375	1.945		27.61	24.527	3.083
30	(C+FA+SF) + (GIF+PPF),	54.92	54.865	0.055	(C+FA+SF) + (GIF+PPF),	55.18	55.173	0.007
100	Sudden Cooling	54.45	54.587	-0.137	Gradual Cooling	54.74	54.871	-0.131
200		53.99	53.916	0.074		54.28	54.165	0.115
300		53.00	52.715	0.285		53.30	52.954	0.346
400		50.80	50.743	0.057		51.10	51.007	0.093
500		47.80	47.917	-0.117		48.08	48.197	-0.117
600		44.55	44.510	0.040		44.80	44.712	0.088
700		40.78	40.857	-0.077		41.00	40.968	0.032
800		36.80	36.920	-0.120		36.99	37.021	-0.031
900		32.50	32.676	-0.176		32.66	32.674	-0.014
1000		28.11	28.307	-0.197		28.24	28.241	-0.001

TABLE XIX.
COMPARISON OF EXPERIMENTAL AND ANN PREDICTED SPLIT TENSILE STRENGTH RESULTS FOR ALL THE CONCRETE COMBINATIONS WITH BOTH COOLING REGIMES

		Split Tensile Strength				Split Tensile Strength		
Sustained Elevated Temperature (°C) [T]	**Combination**	**Experimental Result (MPa) [f_{te}]**	**Predicted Result (MPa) [f_{tp}]**	**% Error**	**Combination**	**Experimental Result (MPa) [f_{te}]**	**Predicted Result (MPa) [f_{tp}]**	**% Error**
30	C, Sudden Cooling	3.86	4.031	-0.171	C, Gradual Cooling	3.98	3.404	0.576
100		3.76	3.759	0.001		3.88	3.646	0.234
200		3.62	3.446	0.174		3.74	3.754	-0.014
300		3.40	3.133	0.267		3.51	3.465	0.045
400		2.96	2.728	0.232		3.06	2.845	0.215
500		2.18	2.178	0.002		2.32	2.188	0.132
600		1.52	1.523	-0.003		1.58	1.722	-0.142
700		0.90	0.901	-0.001		1.12	1.442	-0.322
800		0.43	0.453	-0.023		0.78	1.241	-0.461
900		0.23	0.231	-0.001		0.45	1.039	-0.589
1000		0.00	0.195	-0.195		0.12	0.812	-0.692
30	C + (GIF+PPF),	5.07	5.058	0.012	C + (GIF+PPF),	5.21	5.121	0.089
100	Sudden Cooling	5.00	5.014	-0.014	Gradual Cooling	5.14	5.053	0.087
200		4.92	4.911	0.009		5.06	4.991	0.069
300		4.70	4.683	0.017		4.84	4.850	-0.010
400		4.30	4.300	0.000		4.43	4.551	-0.121
500		3.83	3.775	0.055		3.96	4.077	-0.117
600		3.14	3.157	-0.017		3.24	3.462	-0.222
700		2.52	2.506	0.014		2.62	2.772	-0.152
800		1.88	1.868	0.012		1.94	2.068	-0.128
900		1.32	1.276	0.044		1.40	1.391	0.009
1000		0.74	0.745	-0.005		0.80	0.757	0.043
30	(C+FA+GGBFS) + (GIF+PPF),	6.08	6.075	0.005	(C+FA+GGBFS) +	6.22	6.189	0.031
100	Sudden Cooling	6.01	6.011	-0.001	(GIF+PPF),	6.15	6.082	0.068
200		5.90	5.877	0.023	Gradual Cooling	6.04	5.908	0.132
300		5.60	5.632	-0.032		5.74	5.648	0.092
400		5.26	5.218	0.042		5.40	5.249	0.151
500		4.65	4.658	-0.008		4.78	4.717	0.063
600		4.05	4.067	-0.017		4.15	4.136	0.014
700		3.57	3.536	0.034		3.66	3.604	0.056
800		3.05	3.061	-0.011		3.15	3.159	-0.009
900		2.40	2.607	-0.207		2.50	2.787	-0.287
1000		1.95	2.154	-0.204		2.05	2.454	-0.404
30	(C+FA+SF) + (GIF+PPF),	6.18	6.169	0.011	(C+FA+SF) + (GIF+PPF),	6.28	6.272	0.008
100	Sudden Cooling	6.12	6.134	-0.014	Gradual Cooling	6.23	6.084	0.146
200		6.02	6.019	0.001		6.13	5.897	0.233
300		5.75	5.765	-0.015		5.85	5.648	0.202
400		5.36	5.332	0.028		5.45	5.268	0.182
500		4.75	4.781	-0.031		4.84	4.800	0.040
600		4.18	4.224	-0.044		4.26	4.310	-0.050
700		3.72	3.708	0.012		3.81	3.821	-0.011
800		3.22	3.211	0.009		3.30	3.330	-0.030
900		2.70	2.717	-0.017		2.76	2.846	-0.086
1000		2.26	2.252	0.008		2.31	2.398	-0.088

TABLE XX.
COMPARISON OF EXPERIMENTAL AND ANN PREDICTED WATER ABSORPTION RESULTS FOR ALL THE CONCRETE COMBINATIONS WITH BOTH COOLING REGIMES

		Water Absorption				Water Absorption		
Sustained Elevated Temperature (°C) [T]	**Combination**	**Experimental Result (%) [W_{ae}]**	**Predicted Result (%) [W_{ap}]**	**% Error**	**Combination**	**Experimental Result (%) [W_{ae}]**	**Predicted Result (%) [W_{ap}]**	**% Error**
30	C, Sudden Cooling	1.30	1.297	0.003	C, Gradual Cooling	1.27	1.303	-0.033
100		1.36	1.360	0.000		1.33	1.330	0.000
200		1.45	1.461	-0.011		1.41	1.392	0.018
300		1.58	1.585	-0.005		1.53	1.490	0.040
400		1.75	1.745	0.005		1.65	1.638	0.012
500		1.96	1.961	-0.001		1.85	1.851	-0.001
600		2.26	2.259	0.001		2.15	2.149	0.001
700		2.68	2.681	-0.001		2.57	2.571	-0.001
800		3.25	3.292	-0.042		3.13	3.182	-0.052
900		4.20	4.200	0.000		4.08	4.080	0.000
1000		5.60	5.531	0.069		5.45	5.343	0.107
30	C + (GIF+PPF),	1.08	1.081	-0.001	C + (GIF+PPF),	1.07	1.072	-0.002
100	Sudden Cooling	1.10	1.097	0.003	Gradual Cooling	1.09	1.085	0.005
200		1.13	1.135	-0.005		1.11	1.118	-0.008
300		1.21	1.207	0.003		1.19	1.185	0.005
400		1.34	1.319	0.021		1.32	1.298	0.022
500		1.48	1.478	0.002		1.46	1.458	0.002
600		1.69	1.692	-0.002		1.67	1.672	-0.002
700		1.98	1.979	0.001		1.96	1.959	0.001
800		2.35	2.385	-0.035		2.32	2.363	-0.043
900		2.95	2.990	-0.040		2.92	2.965	-0.045
1000		3.90	3.900	0.000		3.86	3.860	0.000
30	(C+FA+GGBFS) + (GIF+PPF),	0.99	0.991	-0.001	(C+FA+GGBFS) +	0.98	0.980	0.000
100	Sudden Cooling	1.00	1.001	-0.001	(GIF+PPF),	0.99	0.991	-0.001
200		1.03	1.024	0.006	Gradual Cooling	1.01	1.004	0.006
300		1.06	1.071	-0.011		1.03	1.040	-0.010
400		1.15	1.147	0.003		1.11	1.108	0.002
500		1.25	1.246	0.004		1.21	1.205	0.005
600		1.37	1.369	0.001		1.33	1.329	0.001
700		1.51	1.516	-0.006		1.47	1.476	-0.006
800		1.70	1.698	0.002		1.65	1.648	0.002
900		1.95	1.934	0.016		1.88	1.845	0.035
1000		2.29	2.253	0.037		2.17	2.075	0.095
30	(C+FA+SF) + (GIF+PPF),	0.93	0.930	0.000	(C+FA+SF) + (GIF+PPF),	0.92	0.920	0.000
100	Sudden Cooling	0.94	0.941	-0.001	Gradual Cooling	0.92	0.920	0.000
200		0.96	0.958	0.002		0.94	0.938	0.002
300		0.99	0.997	-0.007		0.96	0.980	-0.020
400		1.06	1.063	-0.003		1.04	1.044	-0.004
500		1.16	1.157	0.003		1.13	1.128	0.002
600		1.26	1.271	-0.011		1.23	1.231	-0.001
700		1.40	1.402	-0.002		1.36	1.357	0.003
800		1.56	1.557	0.003		1.51	1.514	-0.004
900		1.76	1.762	-0.002		1.72	1.719	0.001
1000		2.06	2.059	0.001		1.99	1.990	0.000

TABLE XXI.
COMPARISON OF EXPERIMENTAL AND ANN PREDICTED SORPTIVITY RESULTS FOR ALL THE CONCRETE COMBINATIONS WITH BOTH COOLING REGIMES

		Sorptivity				Sorptivity		
Sustained Elevated Temperature (°C) [T]	**Combination**	**Experimental Result ($mm/min^{0.5}$) [S_e]**	**Predicted Result ($mm/min^{0.5}$) [S_p]**	**% Error**	**Combination**	**Experimental Result ($mm/min^{0.5}$) [S_e]**	**Predicted Result ($mm/min^{0.5}$) [S_p]**	**% Error**
30	C, Sudden Cooling	5.49	5.621	-0.131	C, Gradual Cooling	5.40	5.371	0.029
100		5.75	5.807	-0.057		5.65	5.649	0.001
200		6.07	6.139	-0.069		5.96	6.059	-0.099
300		6.50	6.569	-0.069		6.39	6.506	-0.116
400		7.05	7.121	-0.071		6.93	7.022	-0.092
500		7.80	7.824	-0.024		7.66	7.654	0.006
600		8.60	8.709	-0.109		8.44	8.457	-0.017
700		9.68	9.806	-0.126		9.50	9.497	0.003
800		11.08	11.134	-0.054		10.87	10.840	0.030
900		12.80	12.685	0.115		12.55	12.557	-0.007
1000		15.50	14.412	1.088		15.18	14.706	0.474
30	C + (GIF+PPF),	4.30	4.299	0.001	C + (GIF+PPF),	4.25	4.261	-0.011
100	Sudden Cooling	4.47	4.462	0.008	Gradual Cooling	4.41	4.388	0.022
200		4.67	4.676	-0.006		4.61	4.598	0.012
300		4.93	4.917	0.013		4.86	4.883	-0.023
400		5.34	5.240	0.100		5.27	5.272	-0.002
500		5.86	5.697	0.163		5.78	5.773	0.007
600		6.50	6.327	0.173		6.41	6.383	0.027
700		7.20	7.156	0.044		7.10	7.118	-0.018
800		8.16	8.185	-0.025		8.04	8.039	0.001
900		9.35	9.390	-0.040		9.21	9.250	-0.040
1000		11.08	10.714	0.366		10.88	10.877	0.003
30	(C+FA+GGBFS) + (GIF+PPF),	2.88	2.732	0.148	(C+FA+GGBFS) +	2.83	2.826	0.004
100	Sudden Cooling	2.95	2.857	0.093	(GIF+PPF),	2.89	2.897	-0.007
200		3.05	3.005	0.045	Gradual Cooling	2.99	2.990	0.000
300		3.18	3.163	0.017		3.12	3.115	0.005
400		3.36	3.362	-0.002		3.29	3.292	-0.002
500		3.60	3.615	-0.015		3.53	3.528	0.002
600		3.90	3.920	-0.020		3.82	3.822	-0.002
700		4.25	4.271	-0.021		4.17	4.172	-0.002
800		4.67	4.659	0.011		4.58	4.579	0.001
900		5.20	5.079	0.121		5.10	5.044	0.056
1000		5.90	5.530	0.370		5.79	5.572	0.218
30	(C+FA+SF) + (GIF+PPF),	2.52	2.549	-0.029	(C+FA+SF) + (GIF+PPF),	2.47	2.473	-0.003
100	Sudden Cooling	2.57	2.553	0.017	Gradual Cooling	2.51	2.502	0.008
200		2.62	2.604	0.016		2.56	2.567	-0.007
300		2.73	2.702	0.028		2.67	2.661	0.009
400		2.87	2.844	0.026		2.80	2.791	0.009
500		3.02	3.029	-0.009		2.95	2.962	-0.012
600		3.27	3.258	0.012		3.19	3.178	0.012
700		3.54	3.533	0.007		3.46	3.447	0.013
800		3.84	3.860	-0.020		3.76	3.771	-0.011
900		4.25	4.249	0.001		4.16	4.154	0.006
1000		4.70	4.707	-0.007		4.60	4.601	-0.001

TABLE XXII.
COMPARISON OF EXPERIMENTAL AND ANN PREDICTED MODULUS OF ELASTICITY RESULTS FOR ALL THE CONCRETE COMBINATIONS WITH BOTH COOLING REGIMES

Modulus of Elasticity								
Sustained Elevated Temperature (°C) [T]	**Combination**	**Experimental Result x 10^4 (MP_a) [E_{ce}]**	**Predicted Result x 10^4 (MP_a) [E_{cp}]**	**% Error**	**Combination**	**Experimental Result x 10^4 (MP_a) [E_{ce}]**	**Predicted Result x 10^4 (MP_a) [E_{cp}]**	**% Error**
30	C, Sudden Cooling	3.15	3.036	0.114	C, Gradual Cooling	3.25	3.172	0.078
100		3.06	3.055	0.005		3.16	3.160	0.000
200		2.95	2.983	-0.033		3.05	3.070	-0.020
300		2.83	2.808	0.022		2.93	2.899	0.031
400		2.60	2.570	0.030		2.70	2.670	0.030
500		2.30	2.299	0.001		2.40	2.399	0.001
600		2.00	1.995	0.005		2.09	2.091	-0.001
700		1.65	1.652	-0.002		1.75	1.749	0.001
800		1.30	1.292	0.008		1.40	1.392	0.008
900		0.95	0.950	0.000		1.05	1.050	0.000
1000		0.60	0.648	-0.048		0.72	0.757	-0.037
30	C + (GIF+PPF),	4.25	4.245	0.005	C + (GIF+PPF),	4.30	4.298	0.002
100	Sudden Cooling	4.18	4.186	-0.006	Gradual Cooling	4.23	4.236	-0.006
200		4.09	4.079	0.011		4.14	4.129	0.011
300		3.92	3.922	-0.002		3.97	3.978	-0.008
400		3.68	3.697	-0.017		3.73	3.763	-0.033
500		3.42	3.402	0.018		3.47	3.475	-0.005
600		3.06	3.059	0.001		3.13	3.124	0.006
700		2.70	2.702	-0.002		2.74	2.744	-0.004
800		2.35	2.352	-0.002		2.39	2.373	0.017
900		2.01	2.010	0.000		2.05	2.027	0.023
1000		1.65	1.653	-0.003		1.69	1.689	0.001
30	(C+FA+GGBFS) + (GIF+PPF),	4.69	4.696	-0.006	(C+FA+GGBFS) +	4.73	4.728	0.002
100	Sudden Cooling	4.63	4.634	-0.004	(GIF+PPF),	4.67	4.671	-0.001
200		4.56	4.572	-0.012	Gradual Cooling	4.60	4.610	-0.010
300		4.46	4.445	0.015		4.50	4.484	0.016
400		4.20	4.200	0.000		4.24	4.241	-0.001
500		3.86	3.871	-0.011		3.90	3.917	-0.017
600		3.54	3.518	0.022		3.58	3.564	0.016
700		3.16	3.157	0.003		3.19	3.195	-0.005
800		2.78	2.770	0.010		2.81	2.810	0.000
900		2.40	2.347	0.053		2.43	2.423	0.007
1000		2.00	1.897	0.103		2.02	2.063	-0.043
30	(C+FA+SF) + (GIF+PPF),	4.78	4.779	0.001	(C+FA+SF) + (GIF+PPF),	4.81	4.807	0.003
100	Sudden Cooling	4.73	4.730	0.000	Gradual Cooling	4.76	4.768	-0.008
200		4.68	4.675	0.005		4.71	4.705	0.005
300		4.56	4.548	0.012		4.59	4.571	0.019
400		4.32	4.312	0.008		4.35	4.343	0.007
500		4.00	4.003	-0.003		4.03	4.042	-0.012
600		3.66	3.664	-0.004		3.69	3.701	-0.011
700		3.32	3.310	0.010		3.35	3.343	0.007
800		2.94	2.940	0.000		2.97	2.973	-0.003
900		2.56	2.557	0.003		2.59	2.592	-0.002
1000		2.18	2.176	0.004		2.20	2.199	0.001

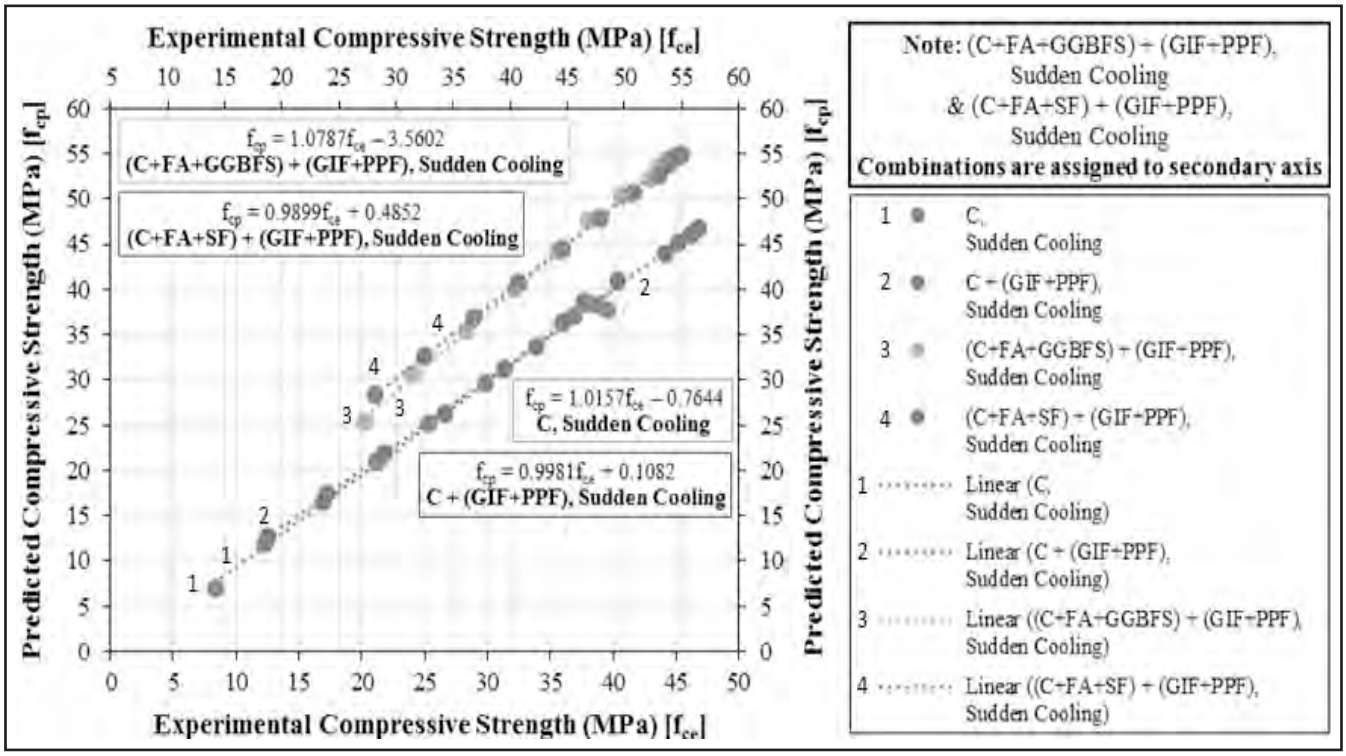

(a)

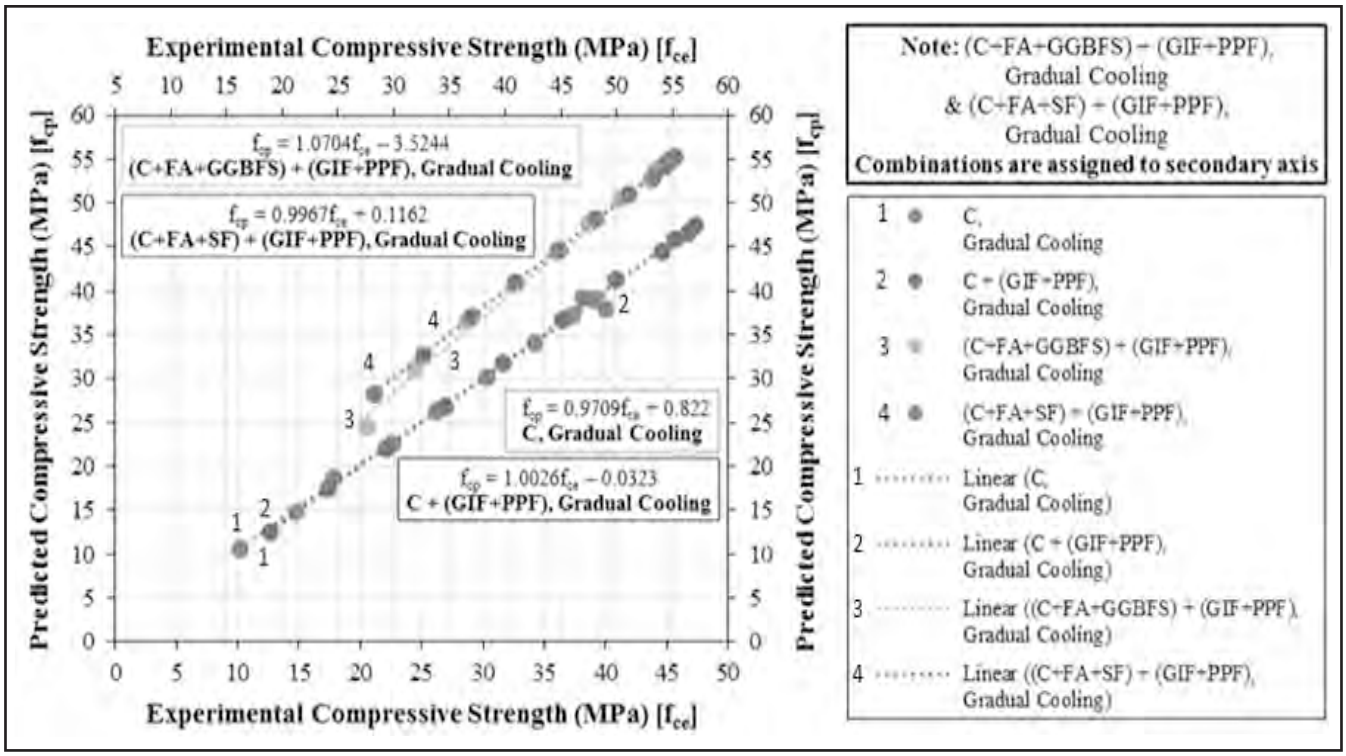

(b)

Fig. 6. Comparison of Experimental and ANN Predicted Compressive Strength Results for all the Concrete Combinations with (a) Sudden Cooling and (b) Gradual Cooling

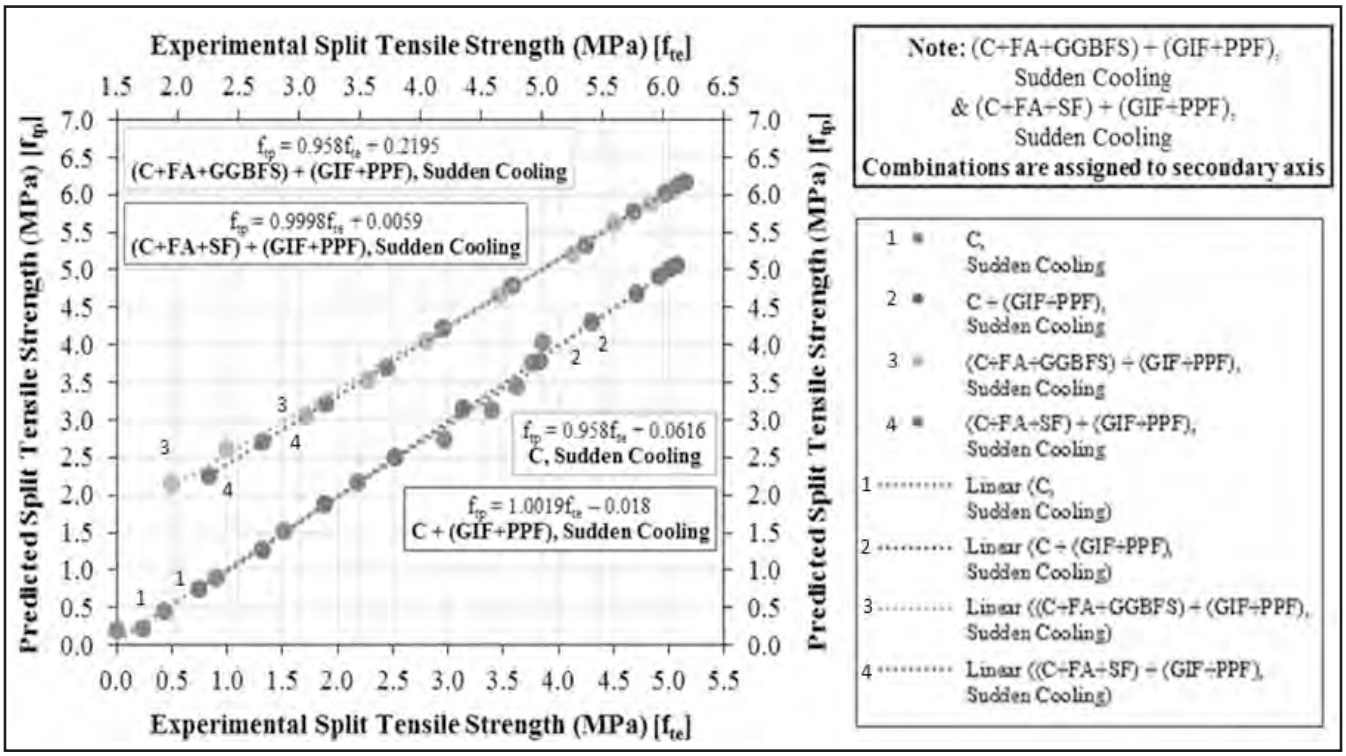

(a)

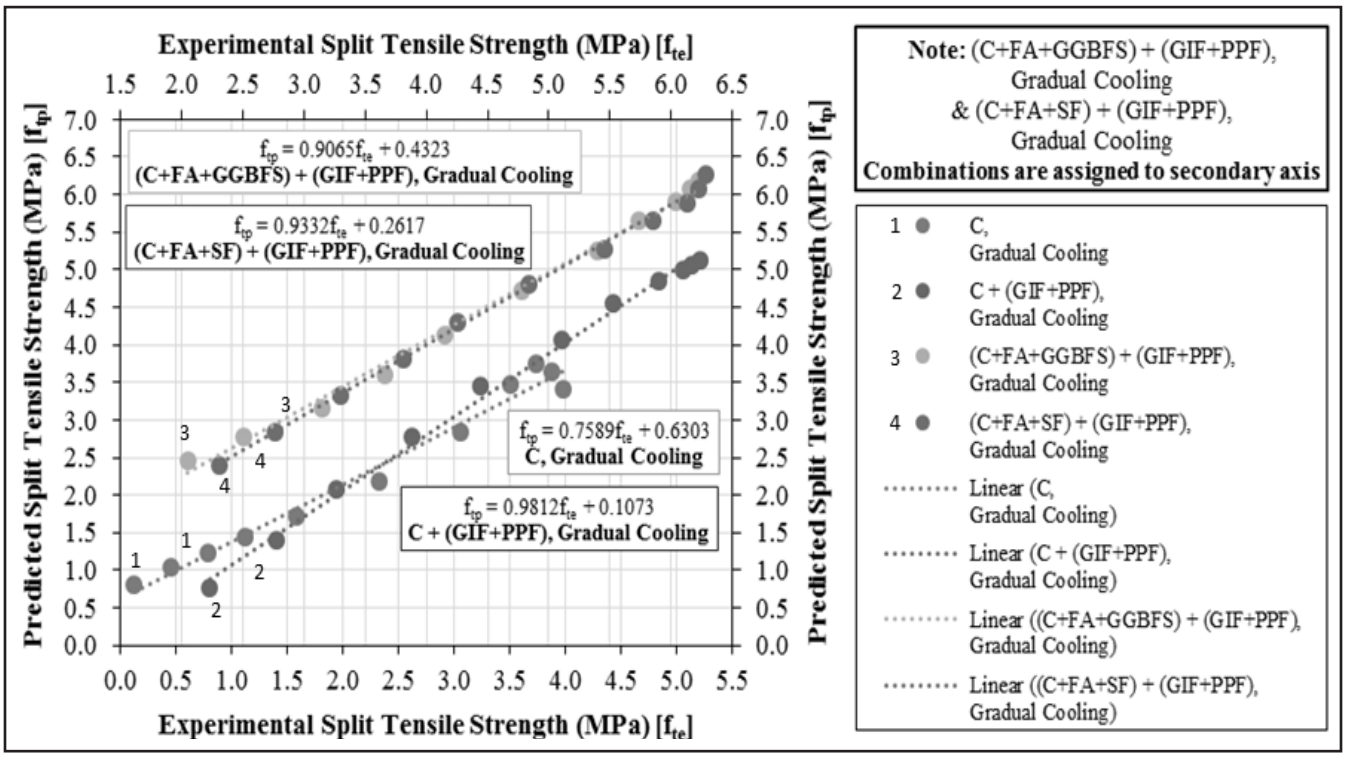

(b)

Fig. 7. Comparison of Experimental and ANN Predicted Split Tensile Strength Results for all the Concrete Combinations with (a) Sudden Cooling and (b) Gradual Cooling

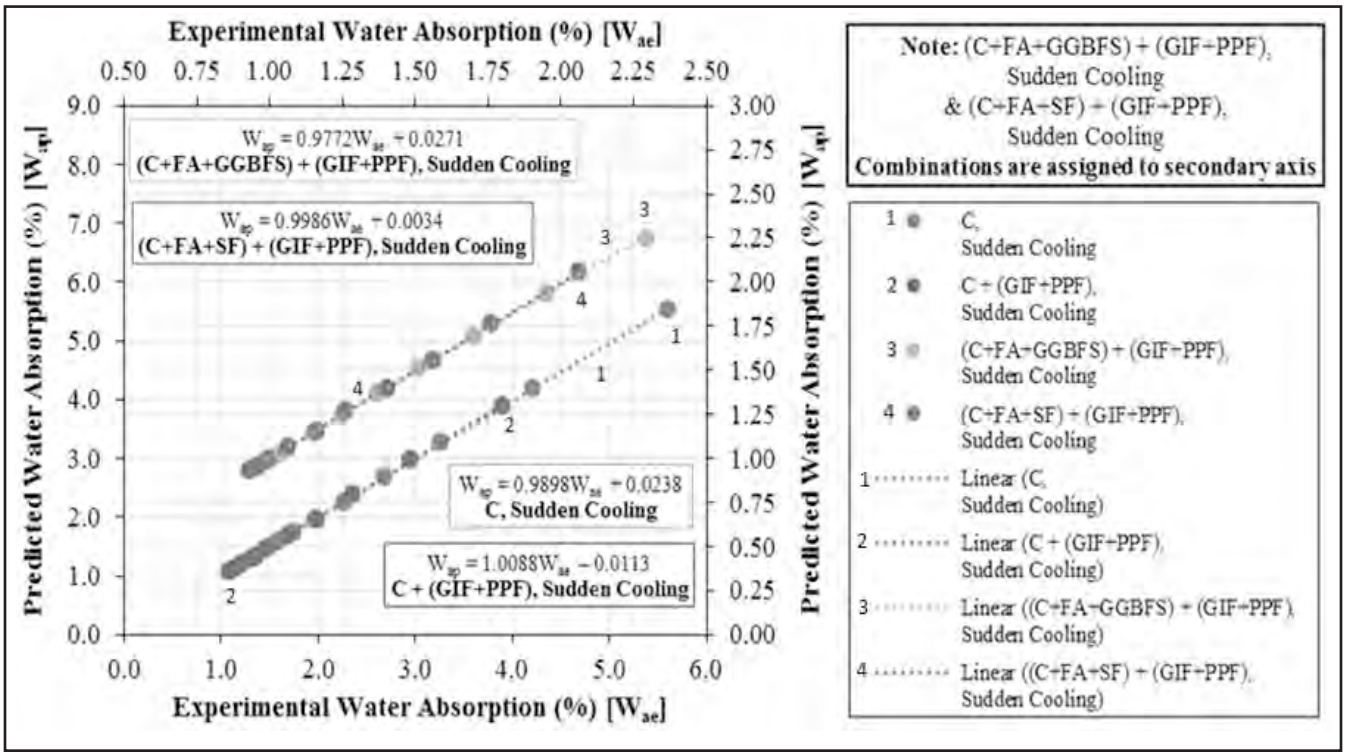

(a)

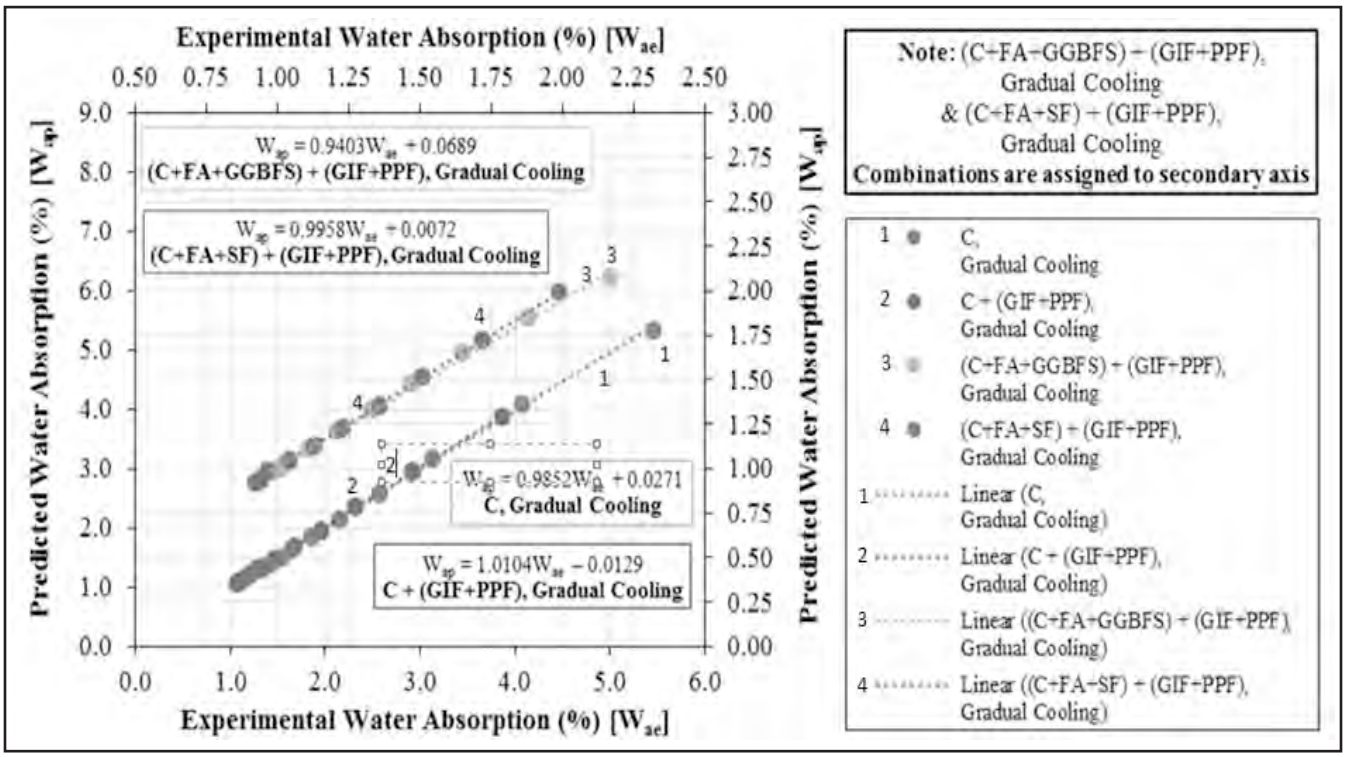

(b)

Fig. 8. Comparison of Experimental and ANN Predicted Water Absorption Results for all the Concrete Combinations with (a) Sudden Cooling and (b) Gradual Cooling

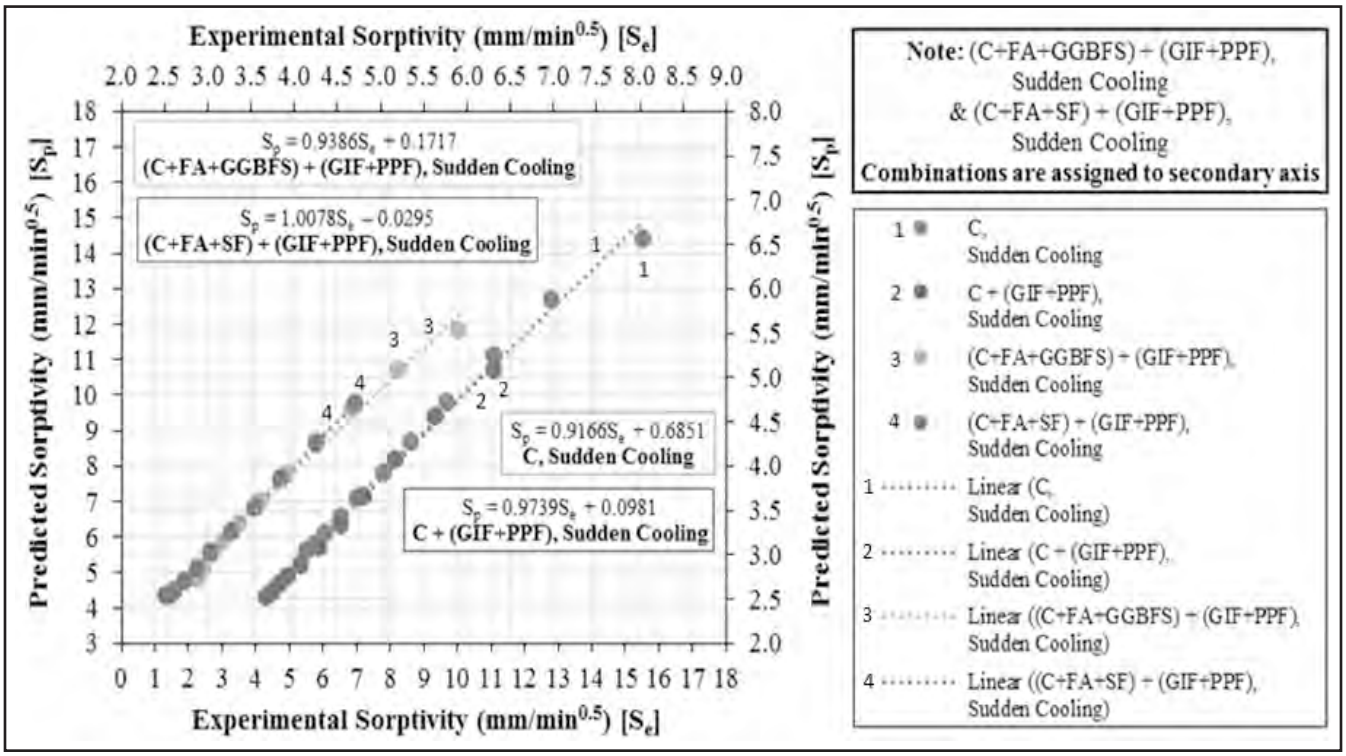

(a)

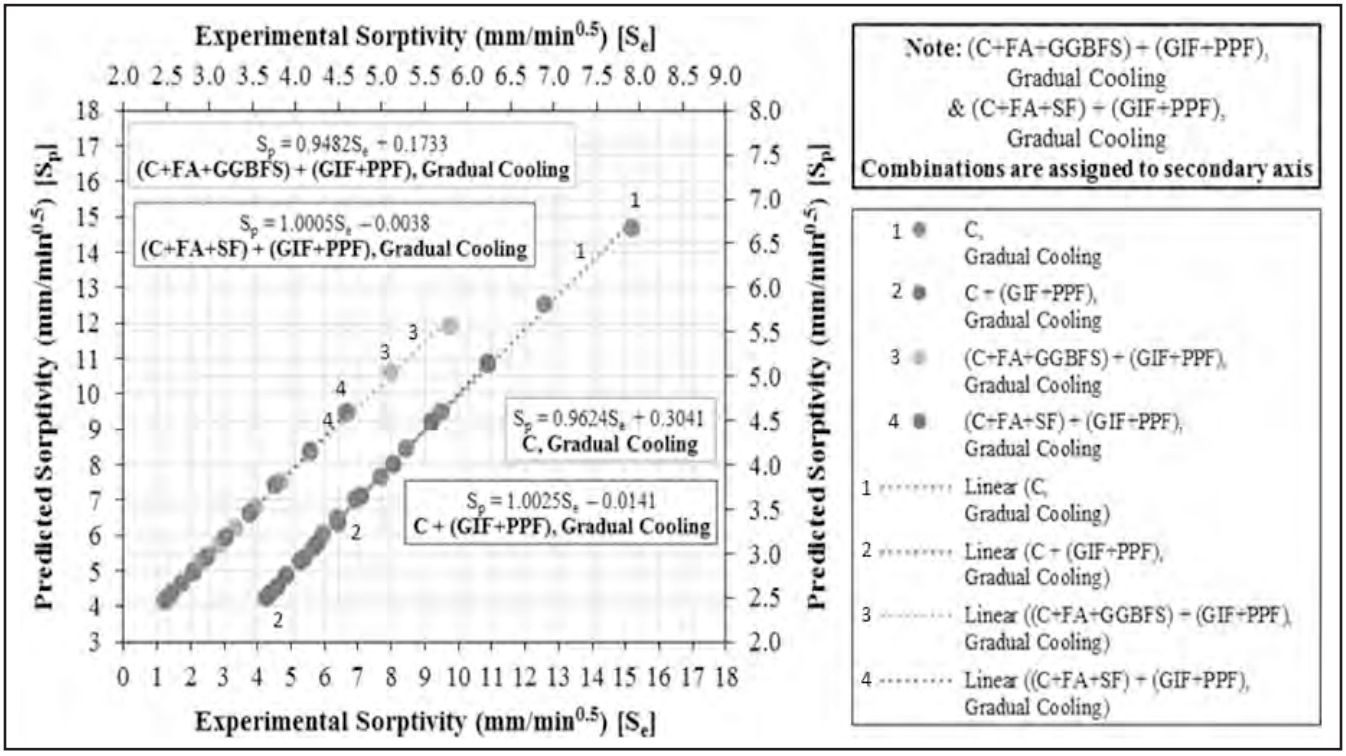

(b)

Fig. 9. Comparison of Experimental and ANN Predicted Sorptivity Results for all the Concrete Combinations with (a) Sudden Cooling and (b) Gradual Cooling

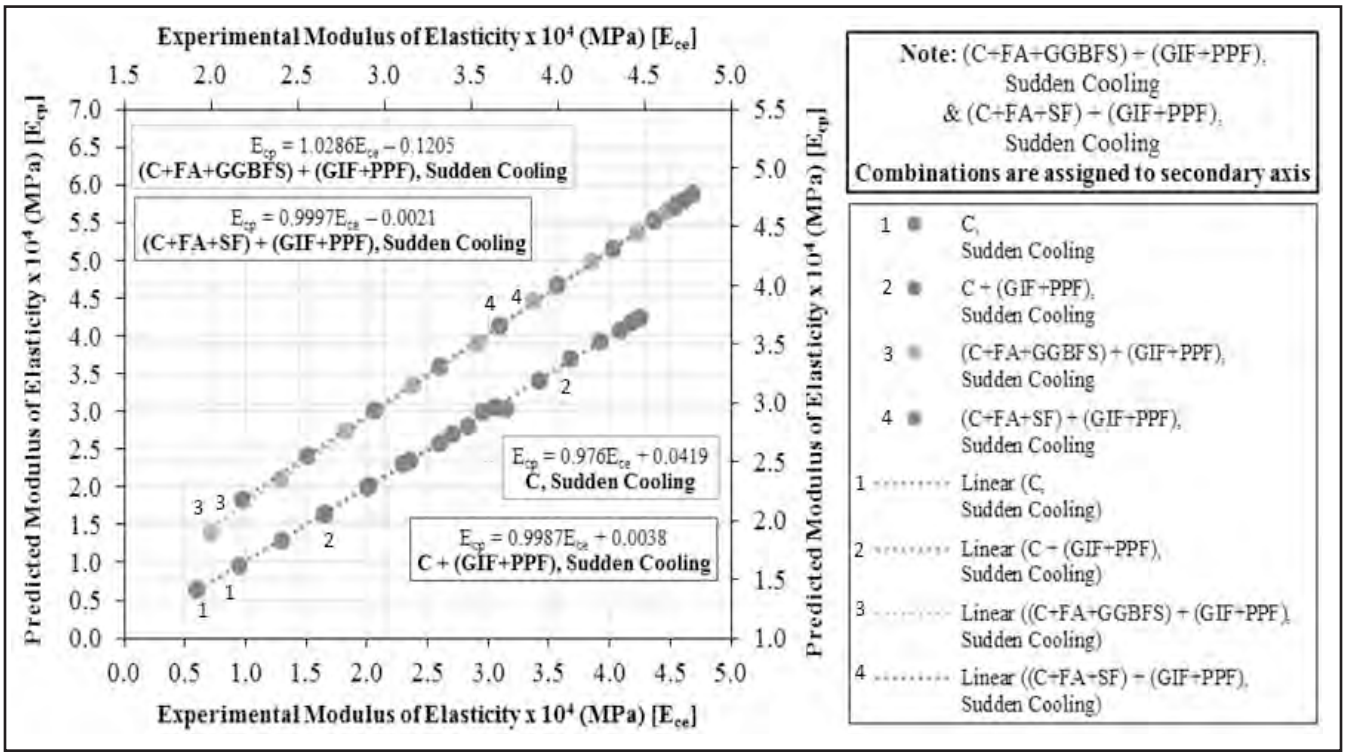

(a)

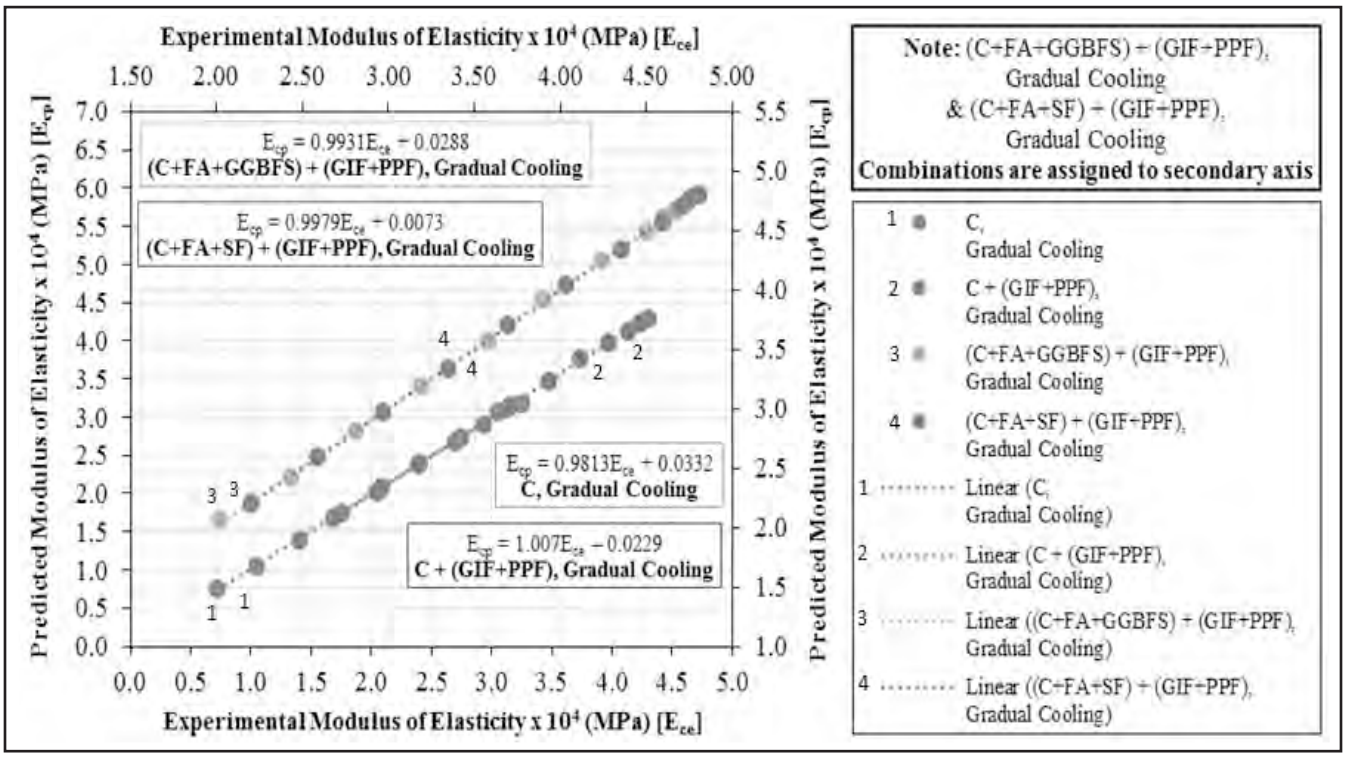

(b)

Fig. 10. Comparison of Experimental and ANN Predicted Modulus of Elasticity Results for all the Concrete Combinations with (a) Sudden Cooling and (b) Gradual Cooling

TABLE XXIII.
STATISTICAL PARAMETERS OF PROPOSED ANN MODELS FOR ALL THE OUTPUTS WITH BOTH COOLING REGIMES

Output Variable	Compressive Strength [f_{cp}]					
	Sudden Cooling [SCR] (Model No. 1)			Gradual Cooling [GCR] (Model No. 2)		
Statistical Parameters	Training Set	Validation Set	Testing Set	Training Set	Validation Set	Testing Set
MSE	0.1015	0.1536	1.3929	0.0184	0.2760	2.1694
RMSE	0.3186	0.3919	1.1802	0.1357	0.5254	1.4729
R^2	0.9997	0.9996	0.9983	0.9999	0.9992	0.9951
Output Variable	**Split Tensile Strength [f_{tp}]**					
	Sudden Cooling [SCR] (Model No. 3)			Gradual Cooling [GCR] (Model No. 4)		
Statistical Parameters	Training Set	Validation Set	Testing Set	Training Set	Validation Set	Testing Set
MSE	0.0003	0.0155	0.0294	0.0275	0.0353	0.1655
RMSE	0.0171	0.1247	0.1715	0.1659	0.1879	0.4068
R^2	1.0000	0.9972	0.9965	0.9972	0.9944	0.9826
Output Variable	**Water Absorption [W_{ap}]**					
	Sudden Cooling [SCR] (Model No. 5)			Gradual Cooling [GCR] (Model No. 6)		
Statistical Parameters	Training Set	Validation Set	Testing Set	Training Set	Validation Set	Testing Set
MSE	1.14e-05	0.0007	0.000976	1.28e-05	0.0012	0.0034
RMSE	0.0034	0.0263	0.0312	0.0036	0.0350	0.0582
R^2	1.0000	1.0000	1.0000	1.0000	0.9998	0.9998
Output Variable	**Sorptivity [S_p]**					
	Sudden Cooling [SCR] (Model No. 7)			Gradual Cooling [GCR] (Model No. 8)		
Statistical Parameters	Training Set	Validation Set	Testing Set	Training Set	Validation Set	Testing Set
MSE	0.0082	0.0059	0.1955	0.0001	0.0037	0.0407
RMSE	0.0908	0.0768	0.4422	0.0108	0.0610	0.2016
R^2	0.9995	0.9996	0.9985	1.0000	0.9997	0.9996
Output Variable	**Modulus of Elasticity [E_{cp}]**					
	Sudden Cooling [SCR] (Model No. 9)			Gradual Cooling [GCR] (Model No. 10)		
Statistical Parameters	Training Set	Validation Set	Testing Set	Training Set	Validation Set	Testing Set
MSE	5.43e-05	0.0003	0.0043	5.17e-05	0.0003	0.0017
RMSE	0.0074	0.0168	0.0656	0.0072	0.0185	0.0407
R^2	1.0000	0.9998	0.9989	1.0000	0.9998	0.9995

the 10 ANN models are within the permissible limits (MSE, RMSE $\cong$ 0 and $R^2 = 1$). The trained models were only tested with the input values and the results found were close to

IV. CONCLUSION

Artificial neural networks are capable of learning and generalizing from examples and experiences. This makes artificial neural networks a powerful tool for solving some of the complicated civil engineering problems.

In this study, using these beneficial properties of artificial neural networks for predicting the compressive strength [f_{cp}], split tensile strength [f_{tp}], water absorption [W_{ap}], sorptivity [S_p], and modulus of elasticity [E_{cp}] without attempting any experiments were developed with 10 different multilayer artificial neural network architectures (Model No. 1 to Model No. 10).

For building ANN models, 440 available experimental results produced with 8 different mixture proportions were used. Two major artificial neural networks were used for prediction. One was for all the concrete combinations with sudden cooling [SCR], and other one is with gradual cooling [GCR]. The data used in the multilayer feed forward neural network models

(architecture, 8–15–1) were designed with eight input parameters covering temperature [T], cement [C], fly ash [FA], GGBFS [GGBFS], Silica Fume [SF], galvanized iron fibre [GIF] polypropylene fibre [PPF], and cooling regime [SCR or GCR]. These five tests were the outputs and they were predicted individually for both the cooling regimes. It shows that neural networks have high potential for predicting results.

It is observed that MSE, RMSE, and R^2 values for all the 10 ANN models are within the permissible limits (MSE, RMSE $\cong$ 0 and $R^2 \cong 1$). The trained models were only tested with the input values, and the results found were close to experiment results.

As a result, successful predictions can be made for strength, near surface characteristics, modulus of elasticity of hybrid fibre reinforced blended concretes subject to sustained elevated temperatures for 3 hours retention period using multilayer feed forward artificial neural networks models without attempting any experiments in a quite short period of time with tiny error rates.

REFERENCES

[1] K. Chandramouli, S. Rao P., N. Pannirselvam, T. S. Sekhar and P. Sravana, "The effect of compressive strength on high strength concrete at different temperature and time," *J. of Emerging Trends in Eng. and App Sci.,* vol. *2*, no. *4*, pp. 698-700, 2011.

[2] A. A. Yaligar and S. B. Vanakudre, "Effect of sudden & gradual cooling regimes on compressive strength of blended concretes subjected to sustained elevated temperatures," *Inter. J. of Inno. Res. in Sci. and Eng*., vol. *2*, no. *5*, pp. 106-15, 2016.

[3] K. S. Rao, Raju M. P. and Raju P. S. N., "Effect of elevated temperatures on compressive strength of HSC made with OPC and PPC," *The Indian Conc. J*., vol. *80*, no. *8*, pp. 43-48, August, 2006.

[4] S. Peter, "Resistance to high temperatures significance of tests and properties of concrete and concrete making materials," *STP 169B ASTM Philadelphia,* 1978, pp. 388-417.

[5] J. Yu, W. Weng, and K. Yu, "Effect of different cooling regimes on the mechanical properties of cementitious composite subjected to high temperatures," *The Scientific World Journal*, pp. 1-7, 2014.
doi: http://dx.doi.org/10.1155/2014/289213

[6] K. S. Kulkarni, S. C. Yaragal, and K. S. B. Narayan, "An overview of high performance concrete at elevated temperatures," *Inter J. of App. Eng. and Tech.,* vol. *1*, no. *1*, pp. 48-60, 2011. [Online]. Available: http://www.cibtech.org/J-ENGINEERING-TECHNOLOGY/PUBLICATIONS/2011/Vol%201%20No.%201/06-08-jet-kulkarni.pdf

[7] A. A. Yaligar and S. B. Vanakudre, "Influence of sudden and gradual cooling regimes on split tensile strength of blended concretes subjected to sustained elevated temperatures," *Inter. J. of Advanced Res. in Sci. and Eng.,* vol. *5*, no. *1*, pp. 118-126, 2016.

[8] Heikal, M., "Effect of elevated temperature on the physico-mechanical and microstructural properties of blended cement pastes," *Build. Res. J.*, vol. *56*, no. 2-3, pp. 157-172, 2008.

[9] K. Venkatesh and R. Nikhil, "Performance of concrete structures under fire hazards: Emerging trends," *The Ind. Conc. J*., April-June, pp. 7-18, 2010.

[10] J. Bai, S. Wild, J. A. Ware, and B. B. Sabir, "Using neural networks to predict workability of concrete incorporating metakaolin and fly ash," *Adv. in Eng. Software,* no. *34*, no. *11-12*, pp. 663-669, 2003.
doi: https://doi.org/10.1016/S0965-9978(03)00102-9

[11] I. B. Topçu and M. Sar?demir, "Prediction of rubberized concrete properties using artificial neural network and fuzzy logic," *Constr. and Build. Mater.,* vol. *22*, no. *4*, pp. 532-540, 2008.
doi: https://doi.org/10.1016/j.conbuildmat.2006.11.007

[12] I. B. Topçu, and M. Sarıdemir, "Prediction of properties of waste AAC aggregate concrete using artificial neural network," *Comp. Mater. Sci.,* vol. *41,* no. *1*, pp. 117-25, 2007.
doi: https://doi.org/10.1016/j.commatsci.2007.03.010

[13] I. B. Topçu, and M. Sarıdemir, "Prediction of compressive strength of concrete containing fly ash using artificial neural network and fuzzy logic," *Comp. Mater Sci.,* vol. *41,* no. *3*, pp. 305-311, 2008.

[14] M. Pala, E. Özbay, A. Öztas and M. I. Yüce, "Appraisal of long-term effects of fly ash and silica fume on compressive strength of concrete by neural networks," Construction and Building Materials, vol. *21*, no. *2*, pp. 384-394, 2007.
doi: https://doi.org/10.1016/j.conbuildmat.2005.08.009

[15] B. B. Adhikary and H. Mutsuyoshi, "Prediction of shear strength of steel fiber RC beams using neural networks," *Construction and Building Materials*, vol. *20*, no. *9*, pp. 801-811, 2006.
doi: https://doi.org/10.1016/j.conbuildmat.2005.01.047

[16] R. Ince, "Prediction of fracture parameters of concrete by artificial neural networks," *Eng. Fracture Mech,* vol. *71*, no. *15*, pp. 2143-59, 2004.

[17] M. A. Kewalramani and R. Gupta, "Concrete compressive strength prediction using ultrasonic pulse velocity through artificial neural networks," *Auto Constr.,* vol. *15*, no. *3*, pp. 374-379, 2006. doi: https://doi.org/10.1016/j.autcon.2005.07.003
[18] 43 grade ordinary portland cement-specification, IS: 8112-1989.
[19] Specification for portland cement, BS: 12-1996.
[20] Standard specification for portland cement, ASTM C 150 / C 150M.
[21] Specification for coarse and fine aggregates from natural sources for concrete, IS: 383-1970.
[22] Specification for aggregates from natural sources for concrete, BS: 882-1992.
[23] Standard specification for concrete aggregates, ASTM C 33 / C 33M.
[24] Pulverized fuel ash (Part-1), IS: 3812-2013.
[25] Fly ash for concrete: definition, specifications and conformity criteria, BS EN 450-1:2012.
[26] Standard specification for coal fly ash and raw or calcined natural pozzolan for use in concrete, ASTM C 618-15.
[27] Specification for granulated slag for the manufacture of portland slag cement, IS: 12089-1987.
[28] Ground granulated blast furnace slag for use in concrete, mortar and grout: definitions, specifications and conformity criteria, BS EN 15167-1:2006.
[29] Standard specification for ground granulated blast-furnace slag for use in concrete and mortars, ASTM C 989-04.
[30] Silica fume-specification, IS: 15388-2003.
[31] Silica fume for concrete: definitions, requirements and conformity criteria, BS EN 13263-1:2005.
[32] Standard specification for use of silica fume as a mineral admixture in hydraulic-cement concrete, mortar, and grout, ASTM C 1240-15.
[33] Concrete admixtures-specification, IS: 9103-1999.
[34] Concrete admixtures. Specification for accelerating admixtures, retarding admixtures and water reducing admixtures, BS 5075-1:1982.
[35] Standard specification for chemical admixtures for concrete, ASTM C 494 / C 494M-16.
[36] Concrete mix proportioning-guidelines, IS: 10262-2009.
[37] D. A. Sinha, A. K. Verma and K. B. Prakash, "Influence of sustained elevated temperature on characteristic properties of ternary blended steel fibre reinforced concrete," *Ind J. of App Res*., August 2014, vol. 4, no. 8, pp. 224-232, 2014.
[38] Fire resistance tests-elements of building construction, part 2: guidance on measuring uniformity of furnace exposure on test samples, ISO 834-2:2014.
[39] A. N. S. A. Qadi, K. N. B. Mustapha, S. Naganathan and Q. N. S. Al-Kadi, "Effect of polypropylene fibres on fresh and hardened properties of self-compacting concrete at elevated temperatures," *Australian J. of Basic and App Sci*., vol. *51,* no. *10*, pp. 378-384, 2011.
[40] *Methods of tests for strength of concrete,* IS: 516-1959.
[41] *Testing concrete: method for determination of compressive strength of concrete cubes*, BS 1881-116: 1983.
[42] *Standard test method for compressive strength of cylindrical concrete specimens,* ASTM C 39 / C39M. s
[43] *Splitting tensile strength of concrete-method of test,* IS: 5816-1999.
[44] *Testing concrete: method for determination of tensile splitting strength,* BS: 1881 (Part 117)-1983.
[45] *Standard test method for splitting tensile strength of cylindrical concrete specimens,* ASTM C 496 / C496M-11.
[46] A. A. Yaligar, S. Patil and K. B. Prakash, "An experimental investigation on the behaviour of retempered concrete," Intern J. of Eng Res-Online, vol. 1, no. 2, pp. 111-120, 2013.
[47] *Standard test method for static modulus of elasticity and poisson's ratio of concrete in compression,* ASTM C 469 / C469M-14.
[48] M. Y. Rafiq, G. Bugmann and D. J. Easterbrook, "Neural network design for engineering applications," *Comput Struct*, vol. *79*, no. *17,* pp.1541-1552, 2001. doi: https://doi.org/10.1016/S0045-7949(01)00039-6
[49] F. Demir, "Prediction of elastic modulus of normal and high strength concrete by artificial neural network," *Construction and Building Materials*, vol. *22*, no. *7*, pp. 1428-1435, 2008. doi: https://doi.org/10.1016/j.conbuildmat.2007.04.004
[50] M. Y. Mansour, M. Dicleli, J. Y. Lee and J. Zhang, "Predicting the shear strength of reinforced concrete beams using artificial neural network," *Eng. Struct.*, vol. *26*, no. *6*, pp. 781-799, 2004.
[51] A. Mukherjee and S. N. Biswas, "Artificial neural networks prediction of mechanical behaviour of concrete at high temperature," *Nuclear Engineering Design,* vol. *178*, no. *1-2*, pp. 1-11, 1997. doi: https://doi.org/10.1016/S0029-5493(97)00152-0
[52] Wu, X. and Lim, S. Y., "Prediction maximum scour depth at the spur dikes with adaptive neural networks," In *Neural Networks and Combinatorial Optimization in Civil and Structural Eng*. Edinburgh: Civil-Comp Press,

pp. 61-66, 1993.
[53] R. Lippman, "An introduction to computing with neural nets," *IEEE ASSP Magazine*, vol. *4*, no. *2*, doi: 10.1109/MASSP.1987.1165576
[54] D. E. Rumelhart, G. E. Hinton, and R. J. Williams, "Learning internal representations by error propagations, "*Parallel Distributed Processing: Explorations in the Microstructure of Cognition*, vol. *1*, pp. 318-362, 1986. Cambridge: MIT Press.
[55] I. B. Topçu and M. Saridemir, "Prediction of mechanical properties of recycled aggregate concretes containing silica fume using artificial neural networks and fuzzy logic," *Computational Material Science*, vol. *42*, no. *1*, pp. 74-82, 2008. doi: https://doi.org/10.1016/j.commatsci.2007.06.011
[56] Ç. Karatas, A. Sözen, E. Arcaklioglu, and S. Ergüney, "Modelling of yield length in the mould of commercial plastics using artificial neural networks," *Materials & Design,* vol. *28*, no. *1*, pp. 278-286, 2007. doi: https://doi.org/10.1016/j.matdes.2005.06.016

About the Authors

Ashish Ashok Yaligar is presently working as an Assistant Professor in Department of Civil Engineering, S. D. M. College of Engineering & Technology (Karnataka, India, affiliated to Visvesvaraya Technological University, Belagavi), Dharwad. He submitted his Ph. D. thesis to Visvesvaraya Technological University, Belagavi, from S. D. M. College of Engineering & Technology, Dharwad. He Completed his M. Tech. in Structural Engineering from Government Engineering College, Haveri, Karnataka, and B. E. in Civil Engineering from P. D. A. College of Engineering, Kalaburagi, Karnataka. He has five and a half years of research experience and has published five research papers in journals and three research papers in international conferences. His areas of interest are concrete technology, analysis and design of structures etc.

Dr. Shrikant B. Vanakudre is presently working as Principal, S. D. M. College of Engineering & Technology, Dharwad, Karnataka, India. He was Head of the Civil Engineering Department and Dean (IPD) at SDMCET Dharwad. He Completed his B. E. in Civil Engineering from University of Mysore, M. E. in Structures from Shivaji University, and Ph. D. in Structures from Visvesvaraya Technological University, Belagavi. He has around 32 years of teaching experience & has worked as Structural Consultant. He has 10 years of research experience. He has published and presented 40 research papers in national and international journals & conferences. He is guiding 3 research scholars under Doctoral Degree programme. His areas of interest are Concrete Technology, Reliability Analysis, Design of Structures etc.